A Study on Contrast-enhanced Ultrasonography with Second-generation Contrast Agent Sonazoid® for Diagnosis of Liver and Splenic Nodules in Dogs

（第二世代超音波造影剤ソナゾイド®を用いた造影超音波検査による犬の肝臓および脾臓腫瘤の診断に関する研究）

Kensuke Nakamura

Laboratory of Veterinary Internal Medicine

Department of Veterinary Clinical Sciences

Graduate School of Veterinary Medicine

Hokkaido University

Index

General Introduction

Ultrasonography is one of the first modalities that has high sensitivity for detection of the abdominal mass lesion. In many patients, however, ultrasonographic characterization of masses is not possible because of poor specificity (1, 2). Tumor vascularity is important for tumor characterization, and this can be done more accurately with computed tomography (CT) or magnetic resonance imaging (MRI) (3, 4). In humans, contrast-enhanced ultrasonography increases the specificity of mass characterization and has been equated to CT and MRI for detection of tumor vascularity (5). An ultrasound contrast agent is an exogenous substance consisting of gas or air microbubbles that are encapsulated by a shell of different composition. Most ultrasound contrast agents do not diffuse across the endothelium and therefore they are basically blood pool agents. In addition to enabling the evaluation of vascularity, some contrast agents are incorporated by the reticuloendothelial system, thus enhancing the parenchyma of organs such as the liver and spleen after the "vascular phase" (6-8). This parenchymal phase imaging significantly improves the detection rate and the delineation of tumors in liver and spleen, given that malignant tumors have little or no reticuloendothelial system and will appear as hypoechoic defects (9-11).

Levovist®,[a] a first-generation contrast agent, has a parenchymal phase and has been used to detect hepatic tumors in humans (12). However, Levovist® has a contrast effect only at high acoustic power leading to microbubble destruction. Bubble destruction produces a strong but transient contrast effect that has an intense signal. Thus, the duration of contrast enhancement of Levovist® is short, limiting its usefulness (13).

Sonazoid®,[b] a second-generation contrast agent, is a suspension of

microbubbles of a low solubility inert gas and has a contrast effect even at a low power. Then, the bubbles develop nonlinear resonance, resulting in harmonic signals with minimal destruction, and provide a longer duration contrast effect and enable more detailed inspection (14, 15). In addition, because Sonazoid® is incorporated by the reticuloendothelial system and is known to enhance visualization of liver parenchyma after the vascular phase, it is recognized as a suitable agent for parenchymal imaging (14, 15).

In human medicine, Sonazoid®-enhanced ultrasonography allows an accurate diagnosis of hepatic tumors (16-18). It was demonstrated that the diagnostic accuracy of Sonazoid®-enhanced ultrasonography for the differentiation of benign and malignant liver lesions was as high as that of CT and MRI. However, it has not been determined whether Sonazoid®-enhanced ultrasonography could be useful diagnostic tool for the lesion in any other organs, such as spleen, because the use of Sonazoid® is limited to the liver lesion now.

In veterinary medicine, contrast-enhanced ultrasonography has been performed for many organs (19-29). The utility of Sonazoid®, however, has been uncertain in veterinary medicine because most contrast agents used in these studies were blood-pool agents (19-21, 23-26, 29) or first-generation agents (22). Liver and spleen are two organs that are most commonly investigated. Until recently, there were only two reports on the characterization of canine liver lesions with contrast-enhanced ultrasonography (20, 22). Kutara *et al.* (22) indicated that the parenchymal imaging with the first-generation contrast agent Levovist® could be useful for the differentiation between benign and malignant liver lesions. However, there were only 8 clinical dogs included in this study. O'Brien *et al.* (20) demonstrated that the second-generation

contrast agent Definity® and Sonovue® could differentiate the benign and malignant canine liver lesion by the vascular imaging. In canine liver, however, the parenchymal imaging could not be performed with these agents. On the other hand, there were three reports on the characterization of canine splenic lesions (24, 26, 29). These studies demonstrated that the vascular imaging with Sonovue® differentiated the benign and malignant splenic lesions. In canine spleen, however, the parenchymal imaging could not be performed with Sonovue®.

The principal aim of this thesis was to investigate the clinical utility of Sonazoid®-enhanced ultrasonography in veterinary medicine. Firstly, the author determined the effect and duration of Sonazoid® on changes in gray-scale enhancement of canine liver parenchyma and portal vein to establish an appropriate protocol for contrast-enhanced ultrasonography of the canine liver. According to the protocol established in this study, the author evaluated the usefulness of Sonazoid®-enhanced ultrasonography in differentiating between malignant and benign hepatic nodules with clinical patients (Chapter 1). Secondly, the author determined the effect and duration of Sonazoid® on changes in gray-scale enhancement of canine spleen parenchyma, splenic arteries and renal cortex to establish an appropriate protocol for contrast-enhanced ultrasonography of the canine spleen. According to the protocol established in this study, the author evaluated the usefulness of Sonazoid®-enhanced ultrasonography in differentiating between malignant and benign splenic nodules with clinical patients (Chapter 2).

CHAPTER 1

CONTRAST-ENHANCED ULTRASONOGRAPHY FOR DIAGNOSIS OF LIVER NODULES IN DOGS

Introduction

Second-generation contrast agents allow continuous real-time evaluation of progressive contrast enhancement of the macro- and micro-vasculature of the normal liver parenchyma and focal liver lesions during the arterial, portal, and late vascular phases with low acoustic power (a low mechanical index [MI]) (30). The evaluation of the arterial, portal, and parenchymal phases with second-generation contrast agents allows differential diagnosis of focal liver lesions with high accuracy (31-33). Sonazoid® is a suitable agent for parenchymal imaging because it is one of the few second-generation contrast agents phagocytized by Kupffer cells (14, 15, 34). Sonazoid®-enhanced ultrasonography allows an accurate diagnosis of human hepatic tumors (16-18).

In veterinary medicine, liver is the most commonly investigated organ with contrast-enhanced ultrasonography (19-23, 27-29). The utility of Sonazoid®, however, has been uncertain in veterinary medicine because there are only two reports of the use of Sonazoid®-enhanced ultrasonography for canine liver (27, 28). Thus, the purpose of this study in chapter 1 was to determine the appropriate timing for the arterial, portal, and parenchymal phases in the normal canine liver and to evaluate the usefulness of these imaging methods with Sonazoid® in clinical patients with hepatic nodules.

Materials and Methods

Six adult laboratory beagles weighing between 7.5 and 14.5 kg were studied. Each dog was healthy based on physical examination and laboratory data. No focal or diffuse hepatic abnormality was noted in any dog on ultrasonographic evaluation. All procedures involving animals were approved by the Hokkaido University Animal Care and Use Committee.

An ultrasound scanner[c] with a 5-11 MHz broadband linear probe[d] suitable for pulse subtraction imaging was used. The mechanical index was set at 0.2 MI to minimize microbubble destruction. Imaging depth was set at 3-4 cm, depending on the subject and a single focal zone was placed in the deepest part of the display. The B-mode gain was set at 90 dB. Ultrasound imaging was made at 19 to 21 frames per second, and the images were recorded continuously on a hard disk for off-line analysis.

It was estimated that a Sonazoid® dose of 0.12 μl microbubbles/kg would be suitable as a clinical dose, in accordance with the manufacturer's instructions and data from rabbits, in which the liver parenchyma was enhanced at doses ranging from 0.045 to 0.315 μl microbubbles/kg (14). A single bolus of the contrast agent was injected in the cephalic vein through a 22-gauge catheter.

Scanning was performed using only manual restraint. The cranial abdomen was shaved, and the dog was in dorsal recumbency. The liver and portal vein were scanned in one image. Intermittent imaging for several seconds at 0, 1, 2, 3, 4, 5, 6, 7, 8, 9, 10, 15 and 30 min after injection was performed so as to minimize microbubble destruction.

For quantitative analysis, individual ultrasound images were acquired using a video frame grabber. An off-line image analysis system[e] was used for calculating signal

intensity. In this system, the gray-scale level ranged from a mean pixel value (MPV) of 0 to 255. Signal intensity was obtained for the liver parenchyma and portal vein. All data were expressed as mean ± standard deviation.

Statistical analysis was performed using Dunnett's multiple comparison tests to evaluate the difference between pre- and post-injection values of each region and by Student's *t*-test to evaluate the difference between the liver parenchyma and portal vein at the same time. A P value of < 0.05 was considered to be significant. Statistical analysis was performed with a standard computer software program.[f]

Twenty-eight hepatic lesions in 27 canine patients presented to Hokkaido University Veterinary Teaching Hospital were evaluated with Sonazoid®. Inclusion criteria were sonographic evidence of hepatic nodules and histologic or cytologic diagnosis of a liver lesion. An ultrasound scanner[c] with a 5-11 MHz broadband linear probe[d] or a 3.75 MHz convex probe[g] suitable for pulse subtraction imaging was selected according to the depth and size of the lesion. A single focal zone was placed in the deepest part of the lesion. The mechanical index was set at 0.2 MI to minimize microbubble destruction. The gain was set so that few signals from the underlying liver parenchyma were present. The images were recorded for off-line analysis. The cranial abdomen was shaved and the dogs were restrained in dorsal recumbency without sedation. Sonazoid® (0.12 μl microbubbles/kg) was injected in the cephalic vein via an intravenous catheter while scanning the lesion. Real-time imaging was performed during the arterial, portal and parenchymal phases. For arterial and portal imaging, the author scanned the lesion continuously from 0 to 1 min after injection. Then, the parenchymal imaging was obtained at least 7 min after injection. The timing of all 3 phases was defined based on the results from the normal beagle dogs. The echogenicity

of the liver lesion was evaluated as hypoechoic, isoechoic or hyperechoic relative to the surrounding normal liver.

Individual ultrasound images were acquired using a video frame grabber. The relationship between the echogenicity and malignancy of the lesion was analyzed using a two-tailed Fisher's exact test with a level of significance of $P < 0.01$. Statistical analysis was performed with a standard computer software program.[f]

Results

In the beagle dogs, the hepatic arteries were enhanced immediately after injection but the enhancement dispersed rapidly. After arterial enhancement, the portal vein became enhanced followed by the parenchyma. MPV of the parenchyma and portal vein were 65.6 ± 13.2 and 53.1 ± 13.4, respectively. MPV of the portal vein (175.0 ± 25.6) was higher than that of the parenchyma (151.2 ± 13.9) until 1 min after injection ($P < 0.05$) (Fig. 1). The contrast effect decreased abruptly and the MPV at 7 min after injection (63.3 ± 10.2) was not significantly different from baseline (Fig. 1). Contrast enhancement of the parenchyma decreased only slightly ($P < 0.05$) with MPV of 128.7 ± 15.6 being maintained up to 30 min. Thus, the optimal time for parenchymal imaging is from 7 min to 30 min after injection and the optimal time for portal vein imaging is 1 min after injection. The timing of the arterial phase could not be defined based on the change of echogenicity of the hepatic arteries because they were too thin to be assessed. Thus it was defined that the arterial phase as the moment when the echogenicity of the portal vein began to rise (35).

Of the 27 clinical patients with 28 hepatic nodules, 5 dogs had a benign nodule, 21 dogs had a malignant nodule, and 1 dog had both benign and malignant nodules. Histologic examination was available for 20 lesions; 5 were benign nodular hyperplasia and 15 were malignant. The 15 malignancies were comprised of 11 hepatocellular carcinomas, 1 combined hepatocellular and cholangiocellular carcinoma, 1 carcinoid, 1 hemangiosarcoma, and 1 osteosarcoma. Needle aspirates were taken with ultrasound guidance in the other 8 lesions with 6 suspected hemangiosarcomas, 1 lymphoma and 1 nodular hyperplasia. Finally, 16 lesions were diagnosed as malignant tumors, and 6 lesions were diagnosed as benign lesions (Table 1).

During the parenchymal phase, all 6 benign lesions were isoechoic to the surrounding normal liver. On the other hand, 15 of the 16 lesions with a confirmed diagnosis of malignancy were hypoechoic (Figs. 2A-E). This finding was significantly ($P < 0.01$) correlated with malignancy with an accuracy of 95.5% [95% confidence interval (CI), 79.5-95.5%], a sensitivity of 93.8% [95% CI, 82.8-93.8%], a specificity of 100% [95% CI, 70.7-100%], a positive predictive value of 100% [95% CI, 88.3-100%], and a negative predictive value of 85.7% [95% CI, 60.6-85.7%].

During the arterial phase, 5 of the 6 benign lesions were isoechoic. Among the 15 malignant lesions, conversely, only one lesion was isoechoic, 11 lesions were hyperechoic and 3 lesions were hypoechoic. Hyperechogenicity or hypoechogenicity during the arterial phase was also significantly related to malignancy ($P < 0.01$) with an accuracy of 90.5% [95% CI, 72.7-97.3%], a sensitivity of 93.3% [95% CI, 80.9-98.1%], a specificity of 83.3% [95% CI, 52.2-95.3%], a positive predictive value of 93.3% [95% CI, 80.9-98.1%], and a negative predictive value of 83.3% [95% CI, 52.2-95.3%]. During the portal phase, there were no characteristic findings.

The benign nodules were all nodular hyperplasia (n=6). Among them, 5 were diagnosed histologically and one cytologically. In the arterial phase, 5 of the nodular hyperplasias were isoechoic to the surrounding liver (Figs. 3A and B). In the portal phase, 5 remained isoechoic and one became hyperechoic. In the parenchymal phase, all 6 were isoechoic, defined as contrast enhancement (Fig. 3C).

Hepatocellular carcinoma (n=11) was the most common malignant tumor. Immediately after injection of Sonazoid®, the branching vasculature became enhanced momentarily in 9 of these 11 dogs (Fig. 4A). In 9 of the 11 dogs, nodules were hyperechoic to the surrounding normal liver during the arterial phase (Fig. 4B). In one

dog, the nodule was hypoechoic to the surrounding normal liver during the arterial phase. In the portal phase, there were no characteristic findings. In the parenchymal phase, 10 of the 11 nodules were hypoechoic (Figs. 2A and 4C). Only one dog had an isoechoic nodule, defined as contrast enhancement.

One dog had a combined hepatocellular and cholangiocellular carcinoma. The nodule was hyperechoic during the arterial phase, then became hypoechoic during the parenchymal phase (Fig. 2B). One dog had a carcinoid. There were multiple small nodules in the liver in this patient. These nodules were hyperechoic during the arterial phase, then hypoechoic in the parenchymal phase (Fig. 2C). One dog had histologically proven hemangiosarcoma. The nodule was hypoechoic during all phases (Figs. 5A-C). Hemangiosarcoma was suspected in 6 other dogs based on cytology; none of these nodules were enhanced during any phase. One dog had a hepatic osteosarcoma. This lesion was hypoechoic to the surrounding normal liver during all three phases (Fig. 2D). One dog had lymphoma and, using conventional ultrasonography, some nodules could not be recognized. Evaluation of the vascular phase was not possible because of patient motion. During the parenchymal phase, multiple hypoechoic nodules were detected (Fig. 2E).

Discussion

In normal dogs, Sonazoid® led to enhanced signal from the portal vein and hepatic parenchyma immediately after injection. Uniform contrast enhancement was maintained for at least 30 min in the liver parenchyma. The signal intensity from the portal vein was the highest at 1 min after injection and then enhancement of the portal vein decreased gradually and disappeared at 7 min after injection. On the basis of these findings, the portal phase was defined as 1 min after injection and the parenchymal phase as 7 to 30 min after injection. Hepatic arteries were too thin to evaluate. However, the time at which echogenicity of the portal vein begins to rise is within the arterial phase (35). Thus the arterial phase was defined as the moment when the echogenicity of the portal vein started to rise.

In clinical patients, malignant nodules were clearly filling defects following Sonazoid® injection. This agrees with findings from humans (16-18). Parenchymal enhancement in rat liver following Sonazoid® injection is due to the distribution of the microbubbles in the Kupffer cells and not in the sinusoids (34). The filling defect during the parenchymal phase created by the malignant nodule is then due to a decrease in the number of Kupffer cells.

The findings of this study with regard to hepatocellular carcinoma were not in complete agreement with prior work in the dog (28). In that study, the presence of an incomplete, irregular, or partial defect during the parenchymal phase was characteristic of hepatocellular carcinoma compared to other malignant tumors. This was hypothesized to be due to residual Kupffer cells in hepatocellular carcinoma nodules. In the present study, no hepatocellular carcinoma was heteroechoic and most were homogeneously hypoechoic, similar to other malignant tumors. On the other hand, one

hepatocellular carcinoma was isoechoic, supporting the presence of large numbers of Kupffer cells in that patient. These findings suggest that the number of Kupffer cells in canine hepatocellular carcinoma differs among patients. In humans, it is indicated that the echogenicity during the parenchymal phase changes from isoechoic to hypoechoic through heteroechoic with progression of histologic grades (18). Additionally, some studies revealed that Kupffer cells were present in human early stage and well-differentiated hepatocellular carcinoma (36-38). Further studies are needed to investigate the relationship between the histologic grade of canine hepatocellular carcinoma and Kupffer cells.

Arterial imaging was also useful to differentiate between malignant and benign lesions. In the present study, nodular hyperplasia was isoechoic and hepatocellular carcinoma was hyperechoic during the arterial phase. These findings agreed with those of previous studies (20, 28). On the other hand, all hemangiosarcomas were hypoechoic during all three phases. This concurred with findings using other ultrasound contrast agents (20, 29) and contrast-enhanced computed tomography (39). In addition to echogenicity, the vasculature patterns during the arterial phase are used to characterize human (16) and canine (28) focal liver lesions. In the present study, hepatocellular carcinoma had a branching vasculature pattern. This agreed with the finding for humans (16), but was incongruent with the finding for dogs (28). The reason for this difference is uncertain. It is quite difficult to evaluate the vasculature pattern accurately because of patient motion and the quite short duration of vasculature enhancement in dogs. Therefore, the vasculature pattern of the canine focal liver lesion should not be overestimated.

There were some limitations in this study. First, because the number of

patients with benign nodules was small, there were large CIs for the specificity and negative predictive value for differentiation between malignant and benign liver lesions. Second, only one hemangiosarcoma was diagnosed histologically. Third, the criteria for diagnosis were not applied prospectively. A prospective study is needed to confirm the accuracy for differential diagnosis of hepatic nodules.

Summary

In 6 normal beagles and 27 dogs with 28 hepatic nodules, contrast-enhanced ultrasonography using Sonazoid® was performed. Sonazoid® is a newly developed second-generation contrast agent with the ability to be used for real-time contrast imaging along with parenchymal imaging. An appropriate protocol for the evaluation of all 3 phases (arterial, portal, and parenchymal) was established based on the results for normal beagles. By evaluation of the echogenicity of hepatic nodules during the arterial and parenchymal phases it was possible to differentiate malignant tumors from benign nodules with very high accuracy. In 15 of 16 nodules diagnosed as malignant tumors, nodules were clearly hypoechoic to the surrounding normal liver during the parenchymal phase. Additionally, malignant tumors had different echogenicity compared to the surrounding normal liver during the arterial phase in 14 of 15 nodules. In the portal phase, there were no characteristic findings. Contrast-enhanced ultrasonography with Sonazoid® appears to improve the characterization of canine focal and multifocal hepatic lesions.

Table and Figures

Table 1. Histological type and contrast enhanced ultrasonographic appearance of the liver lesions of dogs in this study.

Lesion	Mean Size (Range) (cm)	Echogenicity of the liver lesions compared to the surrounding normal liver parenchyma		
		Arterial phase	Portal phase	Parenchymal phase
Malignancy (n=22)				
Epithelial tumor (n=13)				
Hepatocellular carcinoma (n=11)	4.2 (2.0–8.2)	Hyper (n=9), Iso (n=1) Hypo (n=1)	Hyper (n=1), Iso (n=6), Hypo (n=1), Mix (n=3)	Hypo (n=10), Iso (n=1)
Combined hepatocellular cholangiocellular carcinoma (n=1)	1.3	Hyper (n=1)	Mix (n=1)	Hypo (n=1)
Carcinoid (n=1)	multiple (0.5–0.7)	Hyper (n=1)	Hypo (n=1)	Hypo (n=1)
Mesenchymal tumor (n=8)				
Hemangiosarcoma (n=1)	1.7	Hypo (n=1)	Hypo (n=1)	Hypo (n=1)
Osteosarcoma (n=1)	2.5	Hypo (n=1)	Hypo (n=1)	Hypo (n=1)
Hemangiosarcoma suspected (n=6)	4.3 (1.8–8.0)	Hypo (n=6)	Hypo (n=6)	Hypo (n=6)
Hematopoietic tumor (n=1)				
Lymphoma (n=1)	1.8	Not Examined (n=1)	Not Examined (n=1)	Hypo (n=1)
Benignancy (n=6)				
Nodular hyperplasia (n=6)	1.5 (0.5–3.3)	Iso (n=5), Hyper (n=1)	Iso (n=5), Hyper(n=1)	Iso (n=6)

Hyper, hyperechogenicity; Iso, isoechogenicity; Hypo, hypoechogenicity; Mix, mixture.

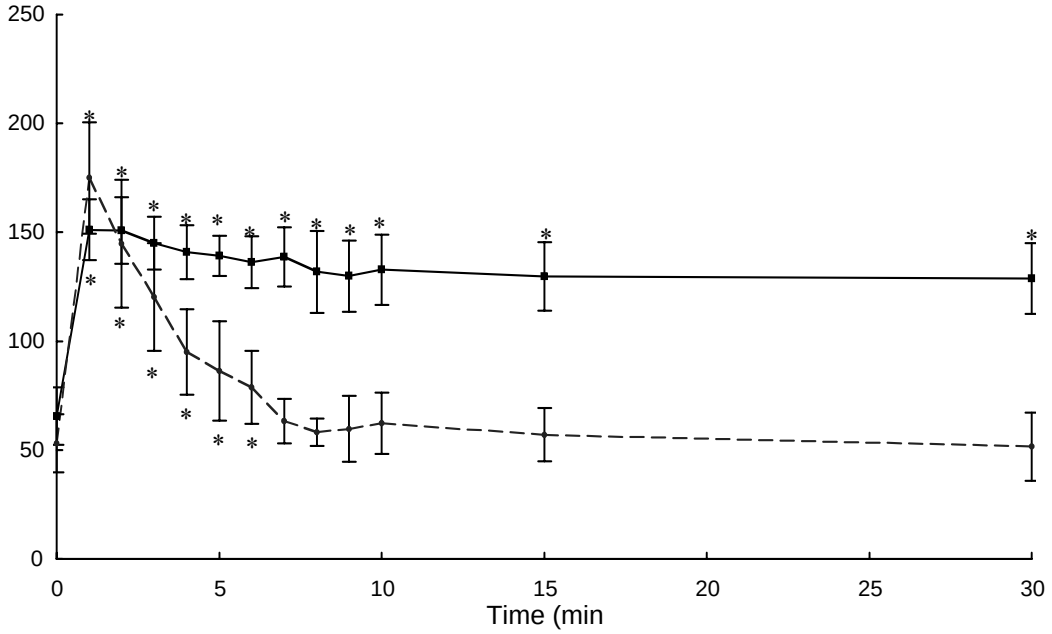

Fig. 1. Time-intensity curves of liver parenchyma (solid line) and portal vein (dotted line) (0 to 30 min after injection of Sonazoid®) in six normal beagles. Bars = standard deviation of the mean.

* Significantly ($P < 0.05$) different from the preinjection values (Dunnett's test).

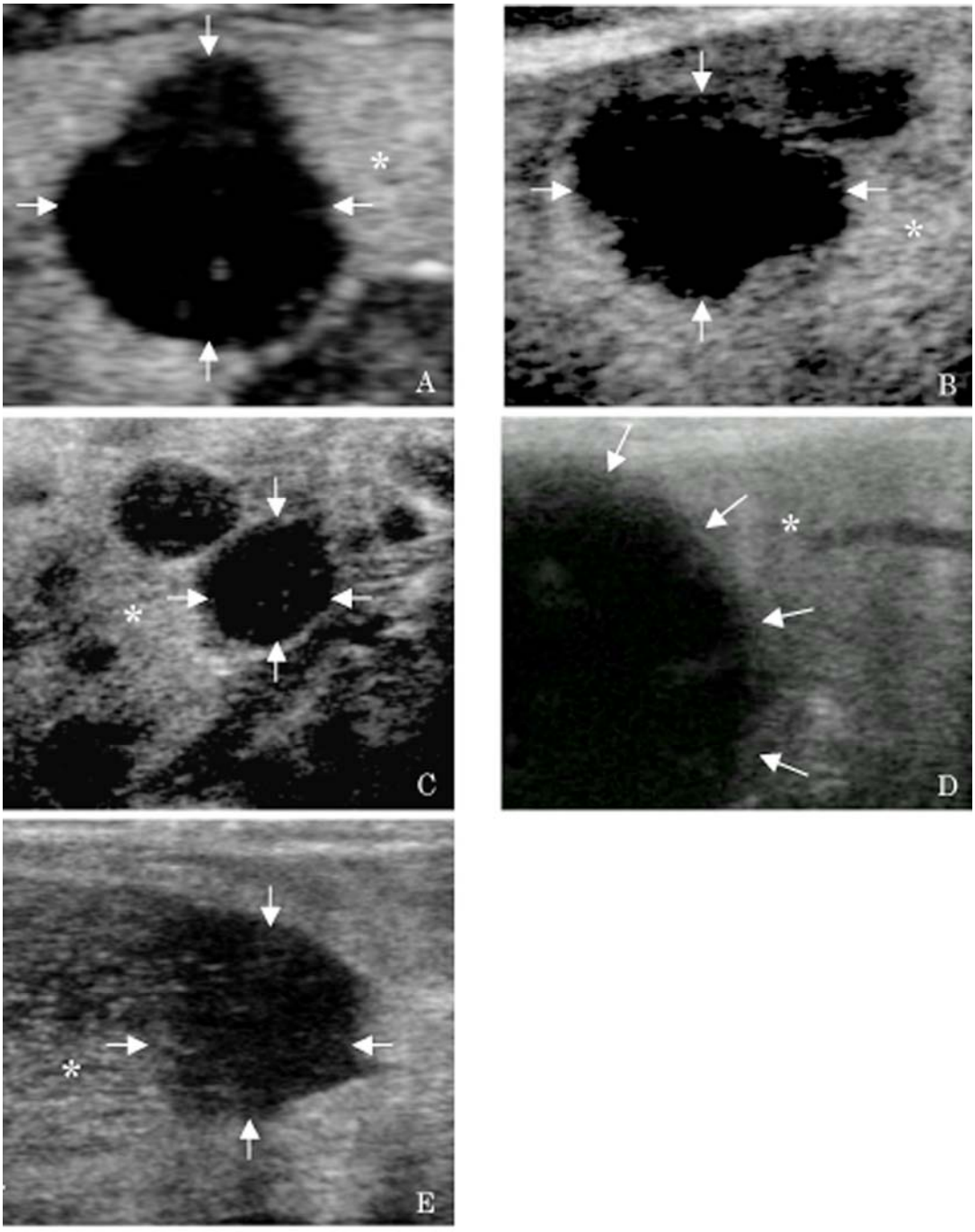

Fig. 2. Ultrasound images of contrast enhancement during the parenchymal phase of hepatic malignant tumors; (A) hepatocellular carcinoma, (B) combined hepatocellular and cholangiocellular carcinoma, (C) carcinoid, (D) hepatic osteosarcoma, (E) lymphoma. All lesions had clear contrast defects (arrows) compared to surrounding normal parenchyma (*).

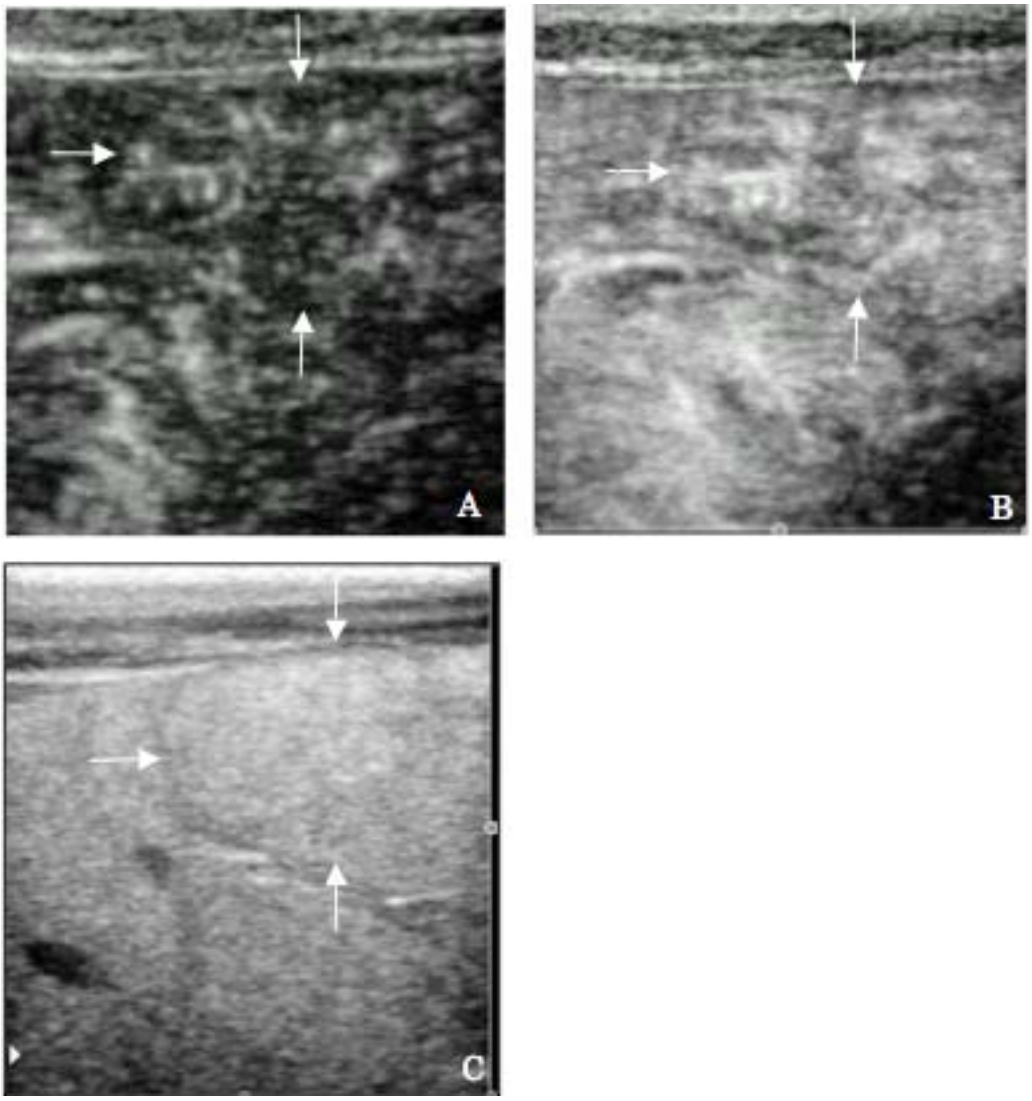

Fig. 3. Ultrasound images of contrast enhancement of nodular hyperplasia. (A) Immediately after injection of Sonazoid®, the vasculature pattern in the lesion was not different from the surrounding normal parenchyma. (B) During the arterial phase, the lesion was isoechoic (arrows) compared to the surrounding normal lesion. (C) During the parenchymal phase, the lesion was isoechoic (arrows).

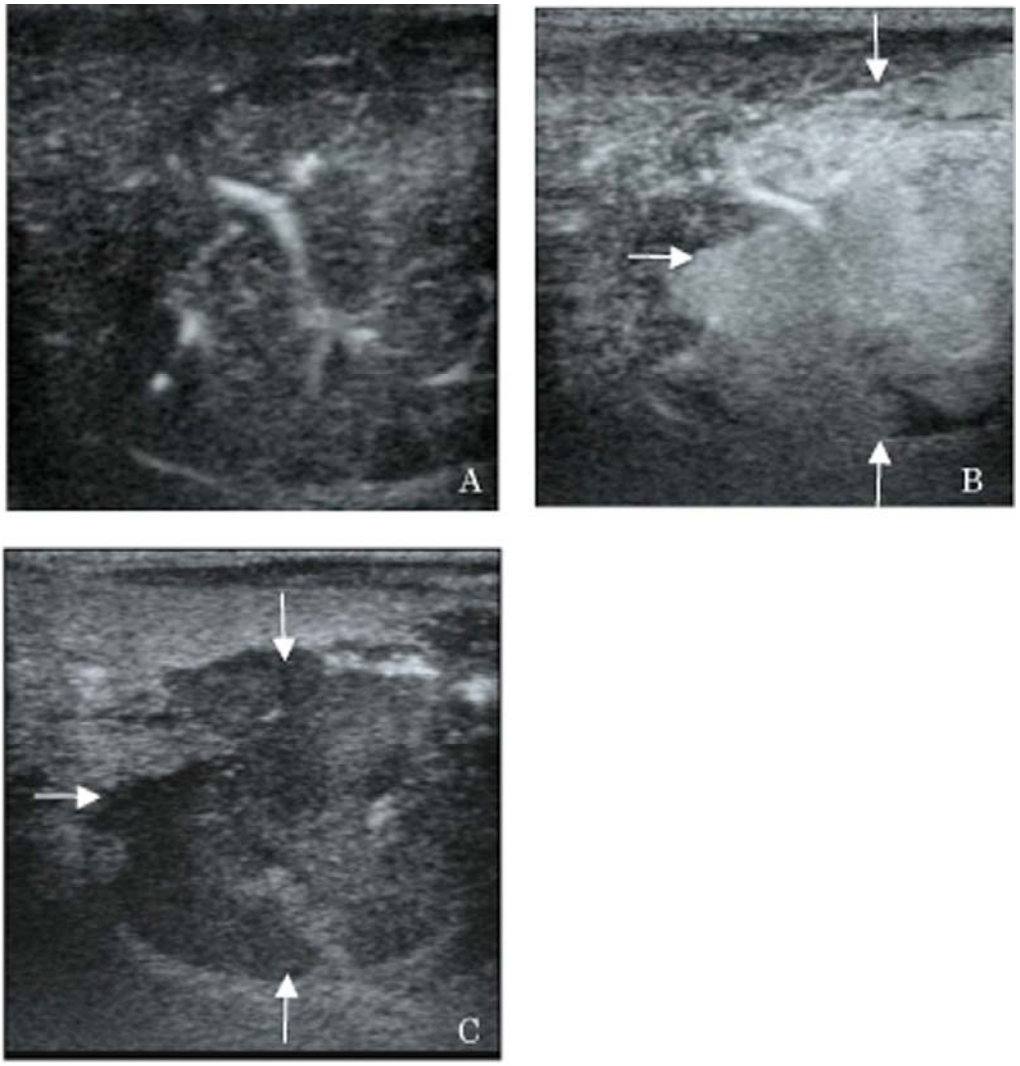

Fig. 4. Ultrasound images of contrast enhancement of hepatocellular carcinoma.

(A) The branching vasculature was enhanced immediately after injection of Sonazoid®. (B) During the arterial phase, the lesion was hyperechoic (arrows) compared to the surrounding normal parenchyma. (C) During the parenchymal phase, the lesion was hypoechoic (arrows).

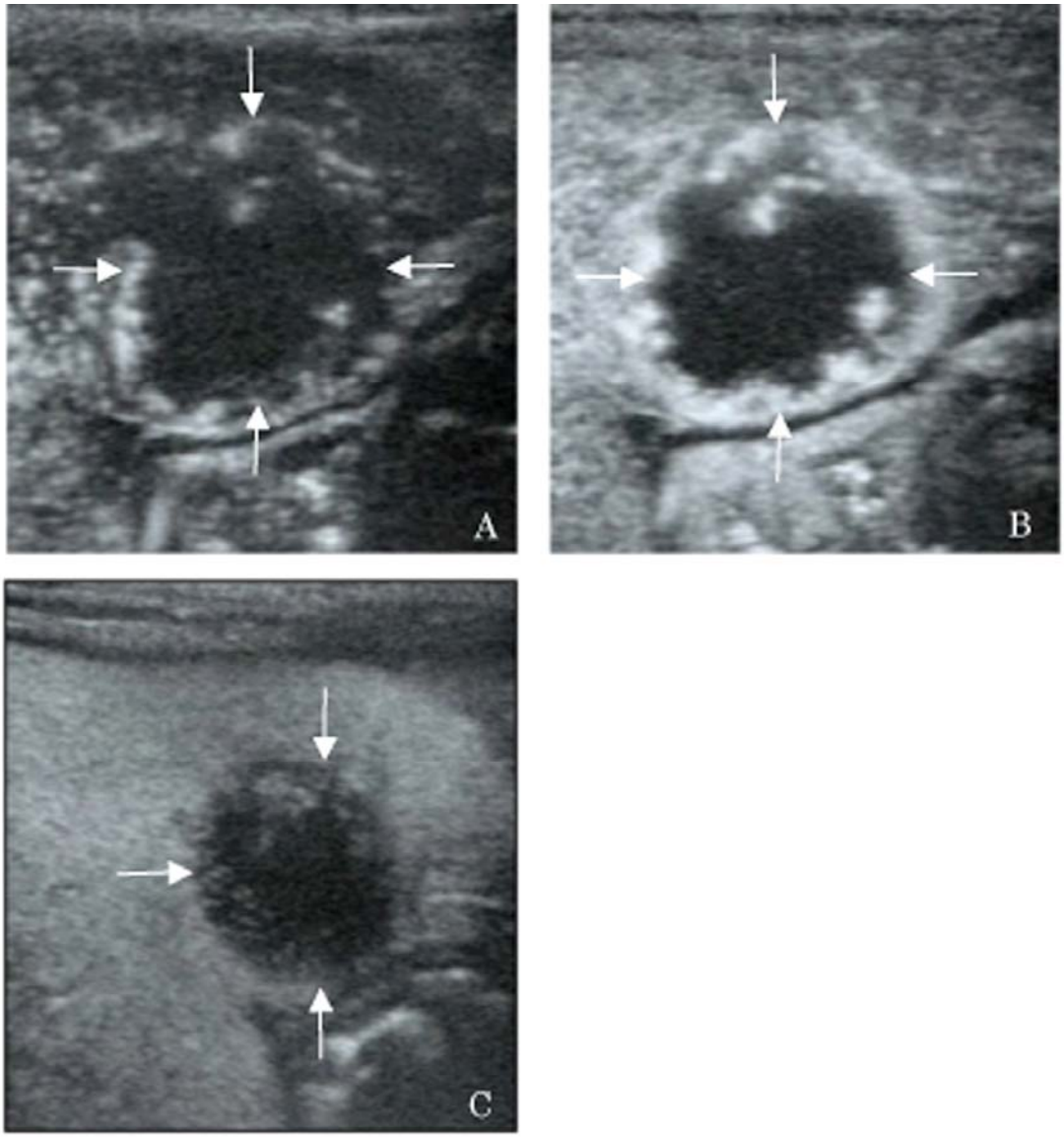

Fig. 5. Ultrasound images of contrast enhancement of hemangiosarcoma. (A) The nodule was not enhanced immediately after injection of Sonazoid®. (B) During the arterial phase, the lesion was hypoechoic (arrows) compared to the surrounding normal parenchyma. (C) During the parenchymal phase, the lesion was hypoechoic (arrows).

CHAPTER 2

CONTRAST-ENHANCED ULTRASONOGRAPHY FOR DIAGNOSIS OF SPLENIC NODULES IN DOGS

Introduction

Ultrasonography is a routine diagnostic procedure for the detection of focal splenic lesions. However, differentiation between benign and malignant lesions is difficult in many cases using conventional ultrasonography, and clear discrimination criteria has not been established yet (40). Therefore, histologic or cytologic examination is necessary to confirm the diagnosis of splenic lesions.

Previous studies showed that contrast-enhanced ultrasonography with second-generation contrast agents could evaluate the tumor perfusion dynamics and improve the differentiation between benign and malignant focal splenic lesions in humans (41) and dogs (24, 26, 29). In addition to vascular imaging, the second-generation contrast agent Sonazoid® is phagocytized by Kupffer cells (34, 42), allowing for long-lasting parenchymal contrast enhancement of the liver (14). Parenchymal imaging improves the diagnostic accuracy to differentiate benign and malignant focal liver lesions in humans (16-18) and dogs (28), given that malignant tumors have little or no reticuloendothelial system and appear as hypoechoic defects.

To date, in humans, three microbubble agents have been characterized as having splenic uptake, i.e., Levovist® (8), Sonovist® (9), and SonoVue® (10). In veterinary medicine, however, no contrast agent has been determined to have spleen parenchyma-specific uptake in dogs. The purpose of this study in chapter 2 was to establish an appropriate protocol for contrast-enhanced ultrasonography of the canine spleen and to determine whether analysis of the enhancement pattern after injection of Sonazoid® would allow to differentiate benign from malignant focal splenic lesions.

Materials and Methods

Six adult laboratory beagles weighing between 7.5 and 14.5 kg were studied. The spleen and left kidney were imaged. The kidney was included for comparison as it has no reticuloendothelial system. Each dog was healthy based on physical examination, and laboratory data. The spleen and kidneys of each dog were sonographically normal. All procedures were approved by the Hokkaido University Animal Care and Use Committee.

Contrast-enhanced ultrasonography was performed with the same ultrasound machine setting as described in chapter 1. A single bolus of Sonazoid® (0.12 μl microbubbles/kg) was injected through a 22-gauge catheter in the cephalic vein. Scanning was performed using only manual restraint. The cranial abdomen was shaved and the dog was in dorsal recumbency. The spleen and left kidney were scanned in one image. For evaluation of the arterial phase, dogs were scanned continuously from pre-injection to 1 min after injection of Sonazoid®. For the parenchymal phase, intermittent imaging for a few seconds at 0, 1, 2, 3, 4, 5, 6, 7, 8, 9, 10, 15 and 30 min after injection was performed so as to minimize microbubble destruction.

For quantitative analysis, individual ultrasound images were acquired by a video frame grabber. An off-line image analysis system[e] was used for calculating videodensity. In this system, the gray-scale level ranged from 0 to 255 MPV. Videodensity was obtained and evaluated for each of three regions of interest, i.e., the normal renal cortex, splenic arteries, and splenic parenchyma. The average baseline values, the average peak values, the time to initial upslope from injection and the time to peak enhancement from initial upslope of all three regions were then calculated. The time of initial upslope was defined as the time when the gray-scale level increased more

than 20 units above baseline because this magnitude of change is generally necessary for visual recognition (14). The average upslope in the spleen was calculated. The data used to calculate the upslope consisted of data points between the initial upslope and peak values. All data were expressed as mean ± standard deviation.

Statistical analysis was performed by using Dunnett's multiple comparison tests to evaluate the difference between pre- and post-injection value of each organ and by Student's *t*-test to evaluate the difference between the spleen parenchyma and arteries at the same time. A P value of < 0.05 was considered to be significant. Statistical analysis was performed with a standard computer software program.[f]

Twenty-nine focal splenic lesions in 29 dogs presented to Hokkaido University Veterinary Teaching Hospital were examined. The study population was recruited from dogs with single or multiple focal splenic lesions detected by conventional ultrasonography. The final diagnosis was confirmed by histology or cytology.

Contrast-enhanced ultrasonography was performed using an ultrasound machine[c] with a 5-11 MHz broadband linear probe[d] or a 3.75 MHz convex probe.[g] A single focal zone was placed at the deepest part of the lesion. The mechanical index was set at 0.1-0.2 MI to minimize microbubble destruction. The gain was set so that few signals from the underlying splenic parenchyma were present. The cranial abdomen was shaved and the dogs were restrained in dorsal recumbency without sedation. Scan planes were chosen to show both a splenic lesion and normal parenchyma in one image. Sonazoid® (0.12 ml microbubbles/kg) was injected via an intravenous catheter in the cephalic vein. Catheters were flushed with saline (0.9% NaCl) solution immediately after the injection. Real-time imaging was performed from preinjection to 1 min after

injection of Sonazoid® for the vascular phases. Images for parenchymal phase were obtained 7-10 minutes after injection according to the results from the normal beagle dogs. All images were recorded on a hard disk for off-line analysis.

Qualitative assessment of the vessel appearance was performed immediately after injection of Sonazoid®. Vessel appearance in lesion was divided into 3 groups in comparison with the vessel in surrounding normal parenchyma: (1) similar, (2) different, and (3) invisible.

Qualitative assessment of the enhancement pattern was performed in the early vascular phase (5-10 sec after injection), late vascular phase (25-30 sec after injection), and parenchymal phase (7-10 min after injection). The timing of all 3 phases was defined based on the results from normal beagle dogs. The contrast enhancement in the surrounding parenchyma was used as an *in vivo* reference. Enhancement pattern were defined subjectively based on echogenicity of lesion parenchyma in comparison with the surrounding normal parenchyma: (1) hypoechoic, (2) isoechoic, and (3) heteroechoic.

Diagnosis was confirmed in all 29 dogs by histology in 24 dogs and ultrasound-guided aspiration cytology in 5 dogs. It was ensured by size and location that the lesions imaged were the ones sampled.

The statistical significance of differences between benign and malignant lesions was calculated with the G-test and two-tailed Fisher's exact test. In addition, the sensitivity and specificity were calculated with 95% CI. $P < 0.05$ was considered significant. Statistical analysis was performed with a standard computer software program.[f]

Results

In the beagle dogs, the renal cortex was characterized by marked enhancement immediately after injection of Sonazoid® in all dogs (Figs. 6A and C). The average baseline value was 19.5 ± 1.3 MPV and the average peak value 158.0 ± 8.3 MPV. Time to initial upslope from injection was 3.6 ± 0.9 sec and the time to peak enhancement from initial upslope 3.6 ± 0.9 sec. The contrast effect decreased abruptly (Fig. 6D) and MPV at 7 min after injection (22.3 ± 2.7) did not differ significantly from the average baseline value (Fig. 7). The mean time when the renal cortex MPV maintained 20 units above baseline was 3.5 ± 0.8 min after injection.

Splenic arteries and parenchyma were characterized by marked enhancement in all dogs immediately after injection (Figs. 6B and 8). Before injection of Sonazoid®, splenic arteries were too thin to be visualized. The splenic vein was, therefore, substituted for evaluation of the average baseline value of splenic arteries. Thus, the derived average baseline value of splenic arteries was 30.2 ± 5.3 MPV and the average peak was 196.9 ± 14.3 MPV. Time to initial upslope from injection of splenic arteries was 5.2 ± 0.4 sec and the time to peak enhancement from initial upslope 2.7 ± 1.0 sec. Subsequent to the enhancement of arteries, the parenchyma was enhanced and arteries became difficult to determine with time (Figs. 6C and D). The gray-scale of splenic arteries was higher than that of the parenchyma for only 5 to 22 sec after injection, but from 23 sec no significant difference was noted between the gray-scale of arteries and that of the parenchyma (Fig. 8).

The average baseline value for the parenchyma was 47.6 ± 6.1 MPV and the average peak value 144.1 ± 9.3 MPV. Time to initial upslope from injection of the parenchyma was 7.0 ± 1.6 sec and the time to peak enhancement from initial upslope

was 20.8 ± 2.1 sec. The average upslope in parenchyma was 3.2 ± 0.7 MPV/sec. Differing dramatically from the contrast enhancement of the renal cortex, contrast enhancement of the splenic parenchyma decreased only slightly and the duration was significant ($P < 0.05$) with a high gray-scale value (107.3 ± 5.3 MPV) maintained up to 30 min (Fig. 7).

According to these results, for Sonazoid® the optimal time for examining the arterial phase of the spleen ranges from 5 to 22 sec after injection and for the parenchymal phase from 7 to 30 min after injection.

Twenty-nine clinical dogs were included. Of the 29 dogs, 13 dogs had benign nodules and 16 dogs had malignant tumors (Table 2).

The vessel appearance was not significantly different between malignant and benign lesions. Similar pattern was found in 9 of the 16 malignant lesions (Fig. 12B) and 10 of the 13 benign lesions (Fig. 9B). Different pattern was found in 4 malignant lesions. In the other 3 malignant and 3 benign lesions, vessel was invisible (Fig. 10B). Among 4 dogs with different pattern, there were 3 hemangiosarcoma and one histiocytic sarcoma. All 3 hemangiosarcoma had aberrant wide or tortuous vessels in nodule (Figs. 11B and C). One histiocytic sarcoma had tortuous vessel. Data for the vessel appearance are given in Table 3.

The enhancement patterns during the early and late vascular phases were significantly different between malignant and benign lesions ($P = 0.02$, and $P < 0.001$, respectively). There was no significant difference during the parenchymal phase. Data for the contrast enhancement pattern after Sonazoid® injection are given in Table 3.

In the early vascular phase, a hypoechoic pattern was found in 6 of the 16 malignant lesions and in none of the 13 benign lesions. All 6 hypoechoic lesions in the

early phase were hemangiosarcoma. Hypoechoic pattern was significantly associated with malignancy (P = 0.02) with sensitivity of 38% [95% CI, 25-38%], and specificity of 100% [95% CI, 84-100%]. An isoechoic pattern was found in 7 of the 16 malignant lesions and 10 of the 13 benign lesions. A heteroechoic pattern was found in 3 of the 16 malignant and 3 of the 13 benign lesions. Isoechoic and heteroechoic pattern were not associated with malignancy or benignancy.

In the late vascular phase, a hypoechoic pattern was found in 13 of the 16 malignant lesions, and 2 of the 13 benign lesions. Hypoechoic pattern in the late phase was significantly associated with malignancy (P = 0.001) with sensitivity of 81% [95% CI, 66-90%], and specificity of 85% [95% CI, 65-95%]. An isoechoic pattern was found in 1 of the 16 malignant lesions, and 9 of the 13 benign lesions. Isoechoic pattern was significantly associated with benignancy (P = 0.001) with sensitivity of 69% [95% CI, 51-76%], and specificity of 94% [95% CI, 79-99%]. A heteroechoic pattern was detected in 2 of the 16 malignant lesions and 2 of the 13 benign lesions. Heteroechoic pattern was not associated with malignancy or benignancy.

In the parenchymal phase, a hypoechoic pattern was found in 15 of the 16 malignant lesions and 11 of the 13 benign lesions. A heteroechoic pattern was found in one malignant lesion and one benign lesion. An isoechoic pattern was found in one benign lesion. There was no significant difference between malignant and benign lesions in the parenchymal phase.

Nodular hyperplasia (n=8) was the most common benign lesion in this study (Figs. 9A-E). In the early vascular phase, 7 of the 8 nodules were isoechoic to the surrounding normal parenchyma (Fig. 9C). In 6 of the 8 dogs, nodules remained isoechoic in the late vascular phase (Fig. 9D). In 2 of the 8 dogs, the nodules became

hypoechoic in the late vascular phase. In the parenchymal phase, all nodules were hypoechoic (Fig. 9E). In two dogs, splenic nodules were diagnosed as hematoma (Figs. 10A-E). In the early and late vascular phases, both nodules were heteroechoic (Figs. 10C and D). In the parenchymal phase, both nodules became homogeneously hypoechoic (Fig. 10E). In two dogs, splenic nodules were diagnosed as extramedurally hematopoiesis. Both nodules were isoechoic during the early and late vascular phases. In the parenchymal phase, one was heteroechoic and another was isoechoic. In one dog, splenic nodule was diagnosed as granuloma. In the early vascular phase, the nodule was isoechoic. It became hypoechoic during the late vascular and parenchymal phase.

Hemangiosarcoma (n=8) was the most common malignant tumor in this study (Figs. 11A-E). In 6 of the 8 dogs, nodules were hypoechoic during the early and late vascular phases. In their nodules, tortuous or aberrant wide vasculature was enhanced but the entire nodules were not enhanced (Figs. 11B-D). In the other two dogs, nodules were heteroechoic in the early and late vascular phases. Seven of the 8 nodules were homogeneously hypoechoic in the parenchymal phase (Fig. 11E) and another was heteroechoic.

Seven of the 8 malignant nodules other than hemangiosarcoma were isoechoic in the early phase (Figs. 12A-C). However, contrast enhancement in these 7 nodules rapidly decreased, and they became hypoechoic in the late vascular phase (Fig. 12D). Finally, all 8 lesions became hypoechoic in the parenchymal phase (Fig. 12E).

Discussion

The results of present study suggest that evaluation of enhancement pattern in Sonazoid®-enhanced ultrasonography has value in differentiating between malignant and benign splenic nodules in dogs with high accuracy. However, the method for differentiating benign and malignant focal splenic lesions was quite different from that for the liver.

The main result of this study in chapter 2 is that there was no significant difference between benign and malignant lesions in the parenchymal phase. This finding is contrary to those of Sonazoid®-enhanced ultrasonography of the liver, in which hypoechogenicity in the parenchymal phase is suggestive of malignant tumors as described in chapter 1. Parenchymal enhancement in the liver following Sonazoid® injection is due to the distribution of the microbubbles in the Kupffer cells (34). The filling defect during the parenchymal phase created by the hepatic malignant tumor is then due to a decrease in the number of Kupffer cells. Conversely, hepatic nodular hyperplasia, the most common benign focal liver lesion in dogs, shows contrast enhancement during the parenchymal phase because the nodules contain Kupffer cells (28, 43). On the other hand, splenic nodular hyperplasia, which is formed by hyperplastic lymphoid cells or mixed accumulations of hyperplastic erythroid, myeloid, and megakaryocytic cells (44), became hypoechoic during the parenchymal phase in the present study. Although the precise mechanism of splenic parenchymal phase imaging is not fully determined, the author speculate that the contrast defect during the parenchymal phase created by splenic nodular hyperplasia might be due to a decrease of splenic macrophages. Therefore, the parenchymal phase imaging was not useful for differentiation between benign and malignant splenic lesions. In some cases, however,

nodules that could not be visualized with conventional ultrasonography became clearly hypoechoic in the parenchymal phase. Therefore, the parenchymal phase imaging could be useful for the detection of focal splenic lesions.

Another important finding is that the detection of hypoechoic nodules in the late vascular phase of Sonazoid®-enhanced ultrasonography is suggestive of malignancy. In contrast, detection of isoechoic nodules in the late vascular phase is suggestive of benign lesions. These findings agree with those of previous studies using the contrast agent SonoVue® (24, 26). SonoVue® is a second-generation contrast agent that has been characterized to have splenic uptake in humans, allowing for parenchymal phase imaging in the human spleen (8). In the canine spleen, however, it was demonstrated that SonoVue® allowed for vascular phase imaging but not for parenchymal phase imaging (24). The vascular phase imaging with SonoVue® could differentiate benign and malignant focal splenic lesions based on the finding that malignant tumors were hypoechoic to the surrounding normal spleen parenchyma in the wash-out phase (30 sec after injection of SonoVue®) (26, 45). In the normal dogs and humans, which have a sinusoidal spleen, a large sieve-like vascular reservoir is formed by an interconnected network of splenic sinusoids and red pulp spaces (44). It has been suggested that some contrast agents are pooled in the splenic sinusoids for a time after intravenous injection (10). Therefore, the author speculates that the lack of normal sinusoids combined with neoplastic angiogenesis might be one of the causes of a malignant hypoechoic pattern during the late vascular phase.

The early vascular phase could also differentiate malignant and benign lesions with high specificity. Among them, hemangiosarcoma showed characteristic hypoechoic pattern during the early vascular phase. This finding concurred with those for

SonoVue®-enhanced ultrasonography (26, 45) and contrast-enhanced computed tomography (39). This hypoechoic area may correspond to the hemorrhagic or necrotic areas commonly associated with hemangiosarcoma. However, differentiation between hemangiosarcoma and hematoma should be done cautiously. In a previous study with the contrast agent Definity®, hemangiosarcoma and hematoma showed similar heteroechoic patterns during the peak enhancement (29). In the present study, likewise, 2 of the 8 hemangiosarcomas and both hematomas had similar heteroechoic patterns during the early vascular phase. Moreover, it was demonstrated that some cases of hematoma exhibited a hypoechoic pattern with SonoVue® (26, 45). Although the exact reasons for these differences are uncertain, it was speculated that they might be due to the differences of contrast agents or patient populations in each study. Further studies are needed to clarify the criteria for discrimination between hemangiosarcoma and hematoma.

Evaluation of vessel appearance has no value in differentiating between malignant tumors and benign nodules. However, although some hemangiosarcomas had aberrant wide vessels, none of the other malignant or benign lesions, including hematoma, had such vessels. This finding agreed with that of a previous study (26). It is quite difficult to evaluate the vessel pattern accurately because of patient motion and the quite short duration of vascular enhancement in dogs. Vasculature pattern of focal canine splenic lesions should be evaluated cautiously but further studies are needed to evaluate its diagnostic significance.

Summary

In 6 normal beagles and 29 dogs with spontaneous focal or multifocal splenic lesions, contrast-enhanced ultrasonography using Sonazoid® was performed. An appropriate protocol for the evaluation of all 3 phases (early vascular, late vascular, and parenchymal) was established based on the results for normal beagles. In 29 dogs with splenic lesions, qualitative assessment of the enhancement pattern was performed in the early vascular, late vascular, and parenchymal phase. In the early vascular phase, a hypoechoic pattern was significantly associated with malignancy (P = 0.02) with sensitivity of 38% [95% CI, 25-38%], and specificity of 100% [95% CI, 84-100%]. In the late vascular phase, a hypoechoic pattern was significantly associated with malignancy (P = 0.001) with sensitivity of 81% [95% CI, 66-90%], and specificity of 85% [95% CI, 65-95%]. There was no significant difference between malignant and benign lesions during the parenchymal phase. In conclusion, there is no significant difference between benign and malignant lesions in the parenchymal phase. Hypoechoic splenic nodules in the early and late vascular phase with Sonazoid®-enhanced ultrasonography is strongly suggestive of malignancy in dogs.

Tables and Figures

Table 2. Clinical data of the 29 dogs with splenic lesions.

Final Diagnosis	n	Median Age (years)	Sex	Distribution	Median Diameter (mm)	Diagnostic Procedure
All dogs	29	11 (3–16)	Male (14), Female (15)	Single (18), Multiple (11)	19.2 (4.4–150.0)	Histology (24), Cytology (5)
Benignancy	13	10 (5–15)	Male (9), Female (4)	Single (8), Multiple (5)	15.0 (4.4–150.0)	Histology (11), Cytology (2)
Nodular hyperplasia	8	8.5 (5–15)	Male (5), Female (3)	Single (5), Multiple (3)	15.0 (6.0–20.9)	Histology (6), Cytology (2)
Hematoma	2	10.5 (7–14)	Male (1), Female (1)	Single (2)	90.0 (29.9–150.0)	Histology (2)
Extramedullary hematopoiesis	2	9.5 (9–10)	Male (2)	Multiple (2)	5.1 (4.4–5.7)	Histology (2)
Granuloma	1	10	Male (1)	Single (1)	10.6	Histology (1)
Malignancy	16	11 (3–16)	Male (5), Female (11)	Single (10), Multiple (6)	26.9 (11.9–73.9)	Histology (13), Cytology (3)
Hemangiosarcoma	8	12 (11–16)	Male (3), Female (5)	Single (8)	37.7 (14.2–73.9)	Histology (8)
Lymphoma	3	5 (3–10)	Male (1), Female (2)	Multiple (3)	22.0 (11.9–31.7)	Cytology (3)
Histiocytic sarcoma	2	9.5 (9–10)	Male (1), Female (1)	Multiple (2)	26.0 (16.0–36.0)	Histology (2)
Leiomyosarcoma	1	14	Female (1)	Single (1)	20	Histology (1)
Osteosarcoma	1	12	Female (1)	Single (1)	35	Histology (1)
Carcinoma	1	11	Female (1)	Multiple (1)	17.5	Histology (1)

Table 3. Contrast enhancement pattern in 29 dogs.

Enhancement pattern	Benign lesions					Malignant lesions						
	All	Nodular hyperplasia	Hematoma	Hemato-poiesis	Granuloma	All	Hemangio-sarcoma	Lymphoma	Histiocytic sarcoma	Leiomyo-sarcoma	Osteo-sarcoma	Carcinoma
n	13	8	2	2	1	16	8	3	2	1	1	1
Vessel appearance												
Similar	10	7	1	1	1	9	3	3	1	1	0	1
Different	0	0	0	0	0	4	3	0	1	0	0	0
Invisible	3	1	1	1	0	3	2	0	0	0	1	0
Early vascular phase[a]												
Hypoechoic	0[d]	0	0	0	0	6[d]	6	0	0	0	0	0
Heteroechoic	3	1	2	0	0	3	2	1	0	0	0	0
Isoechoic	10	7	0	2	1	7	0	2	2	1	1	1
Late vascular phase[b]												
Hypoechoic	2[c]	2	0	0	0	13[c]	6	3	1	1	1	1
Heteroechoic	2	0	2	0	0	2	2	0	0	0	0	0
Isoechoic	9[c]	6	0	2	1	1[c]	0	0	1	0	0	0
Parenchymal phase												
Hypoechoic	11	8	2	0	1	15	7	3	2	1	1	1
Heteroechoic	1	0	0	1	0	1	1	0	0	0	0	0
Isoechoic	1	0	0	1	0	0	0	0	0	0	0	0

[a, b]Significantly different between benign and malignant lesions: [a]$P < .001$. ; [b]$P = .02$. Statistical differences were calculated with G-test.
[c, d]Significantly different between benign and malignant lesions: [c]$P = .001$. ; [d]$P = .02$. Statistical differences were calculated with two-tailed Fisher's exact-test.

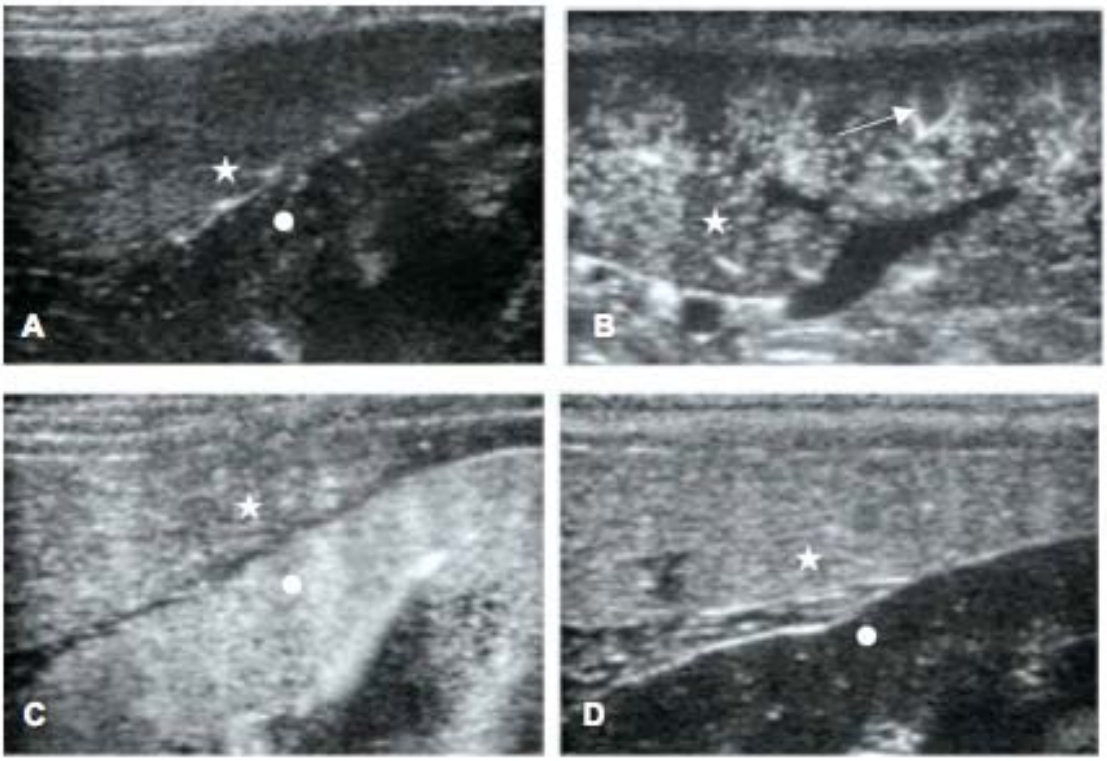

Fig. 6. Longitudinal images of contrast enhancement of a normal spleen (star) and kidney (circle) in a beagle (cranial is to the left, caudal to the right). (A) Image acquired before injection of contrast medium. The probe and machine were preset for contrast harmonic imaging. (B) Contrast-enhanced splenic arteries are seen 5 sec after injection of contrast agent (arrow). (C) Contrast enhancement occurs both in the spleen and kidney (shown here 1 min after injection). (D) Although contrast enhancement of the kidney disappears, persistent enhancement of the spleen is seen (10 min after injection).

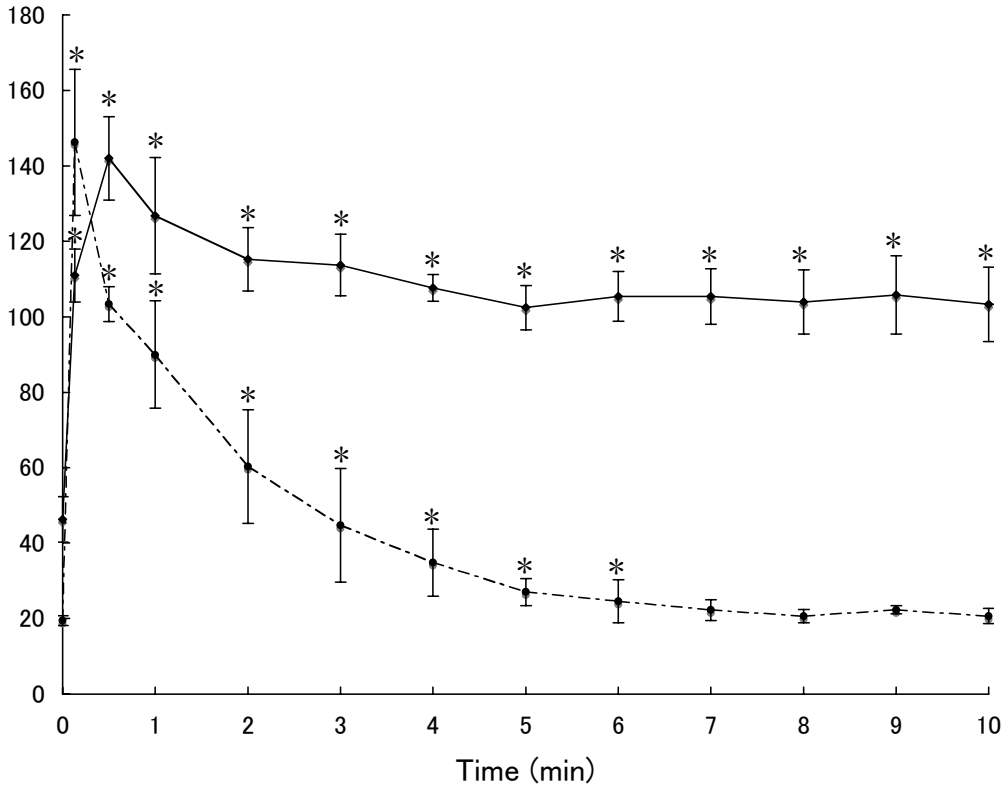

Fig. 7. Time-intensity curves of splenic parenchyma (solid line) and renal cortex (dotted line) in 6 normal beagles (0 to 10 min after injection of Sonazoid®). Bars = standard deviation of the mean.

* Significantly ($P < 0.05$) different from the pre-injection values (Dunnett's test).

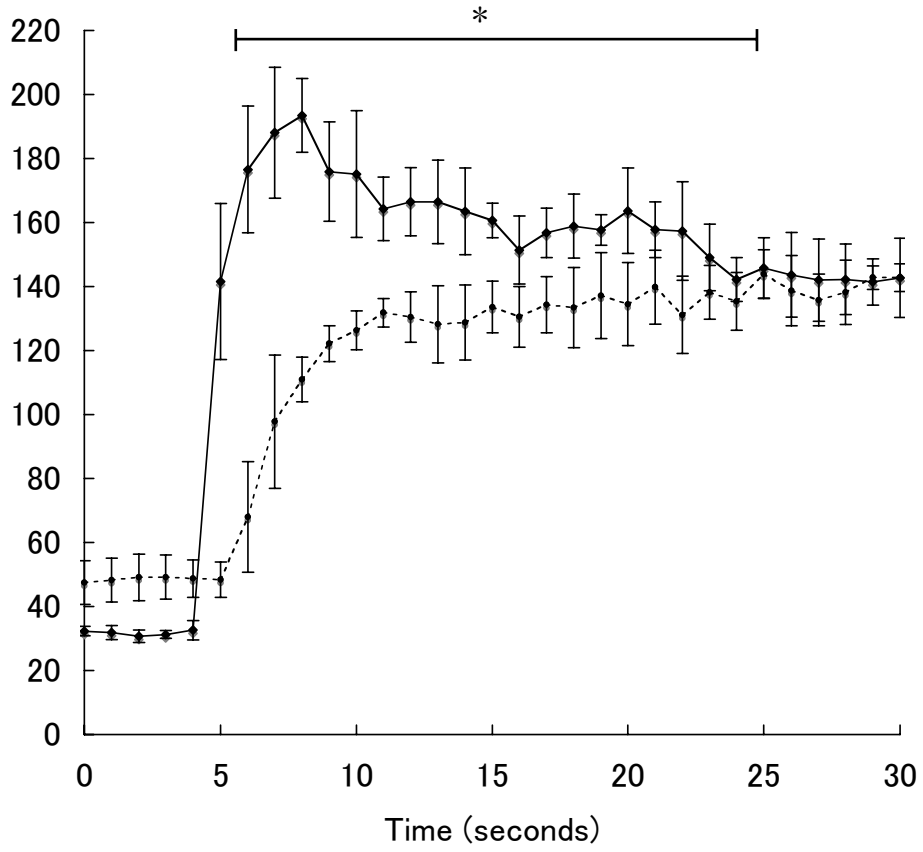

Fig. 8. Time-intensity curves of splenic arteries (solid line) and parenchyma (dotted line) in the early phase (0 to 30 sec after injection of Sonazoid®) in 6 normal beagles. Bars = standard deviation of the mean.

* Significantly ($P < 0.05$) different from the parenchyma at the same time (Student's *t*-test).

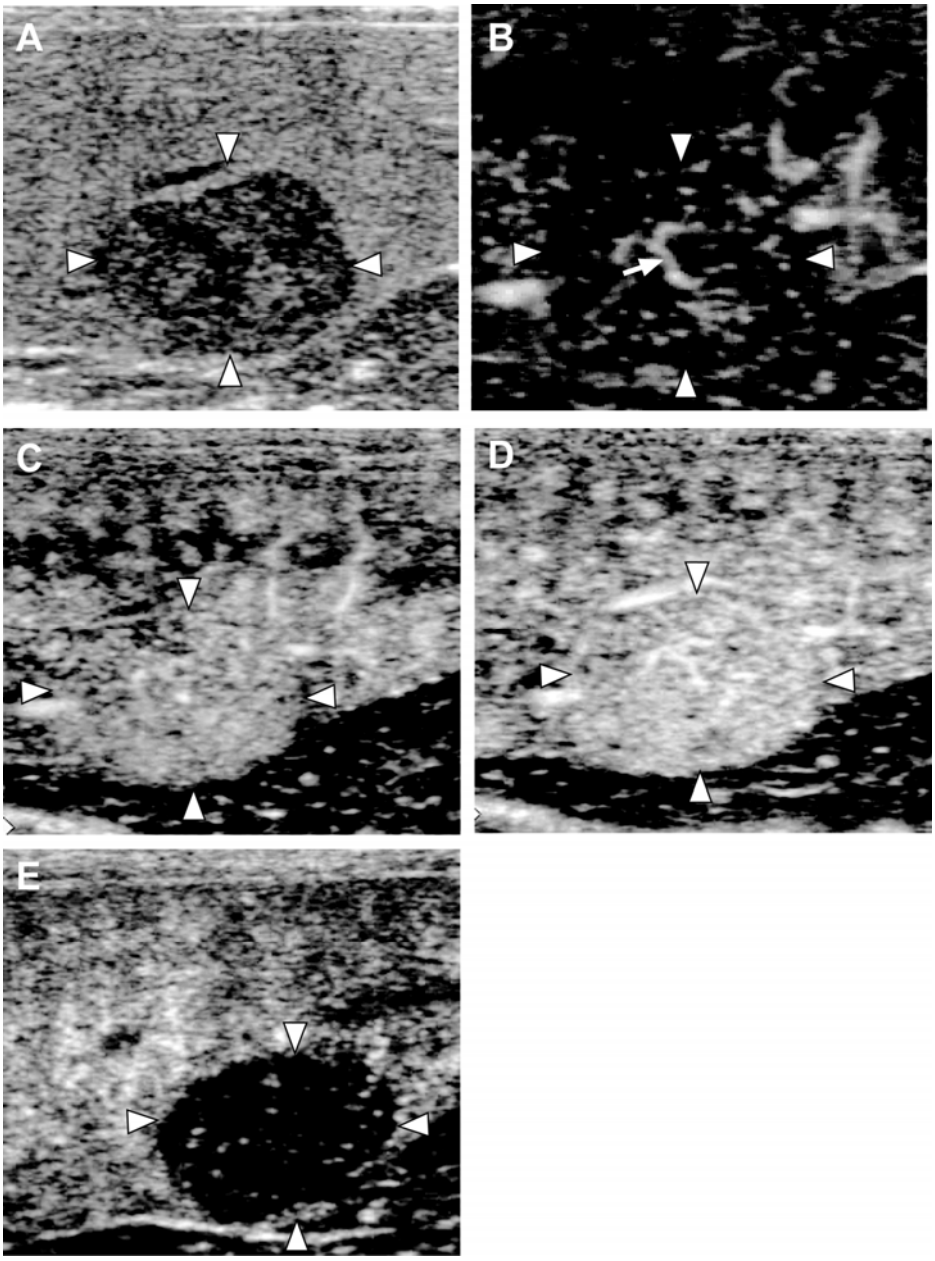

Fig. 9. (A) Conventional ultrasound imaging and (B-E) Sonazoid®-enhanced imagings of splenic nodular hyperplasia. (B) Immediately after injection, the vessel pattern (arrow) in the lesion (arrowheads) was similar to the surrounding parenchyma. During both (C) the early vascular and (D) the late vascular phase, the lesion was isoechoic (arrowheads) compared to the surrounding normal parenchyma. (E) During the parenchymal phase, the lesion became hypoechoic (arrowheads).

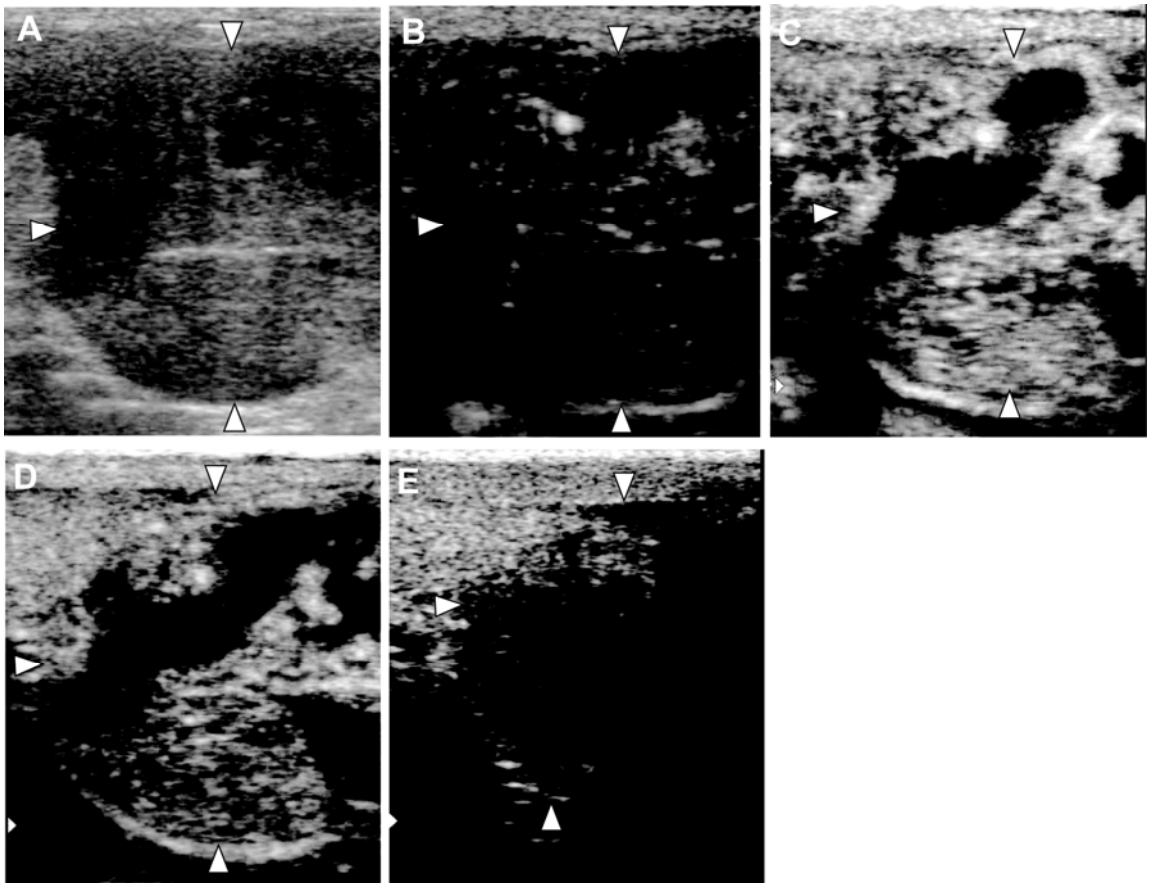

Fig. 10. (A) Conventional ultrasound imaging and (B-E) Sonazoid®-enhanced imagings of splenic hematoma. (B) Immediately after injection, no vessel was visualized in the lesion (arrowheads). During both (C) the early vascular and (D) the late vascular phase, the lesion was heteroechoic (arrowheads). (E) During the parenchymal phase, the lesion became hypoechoic (arrowheads).

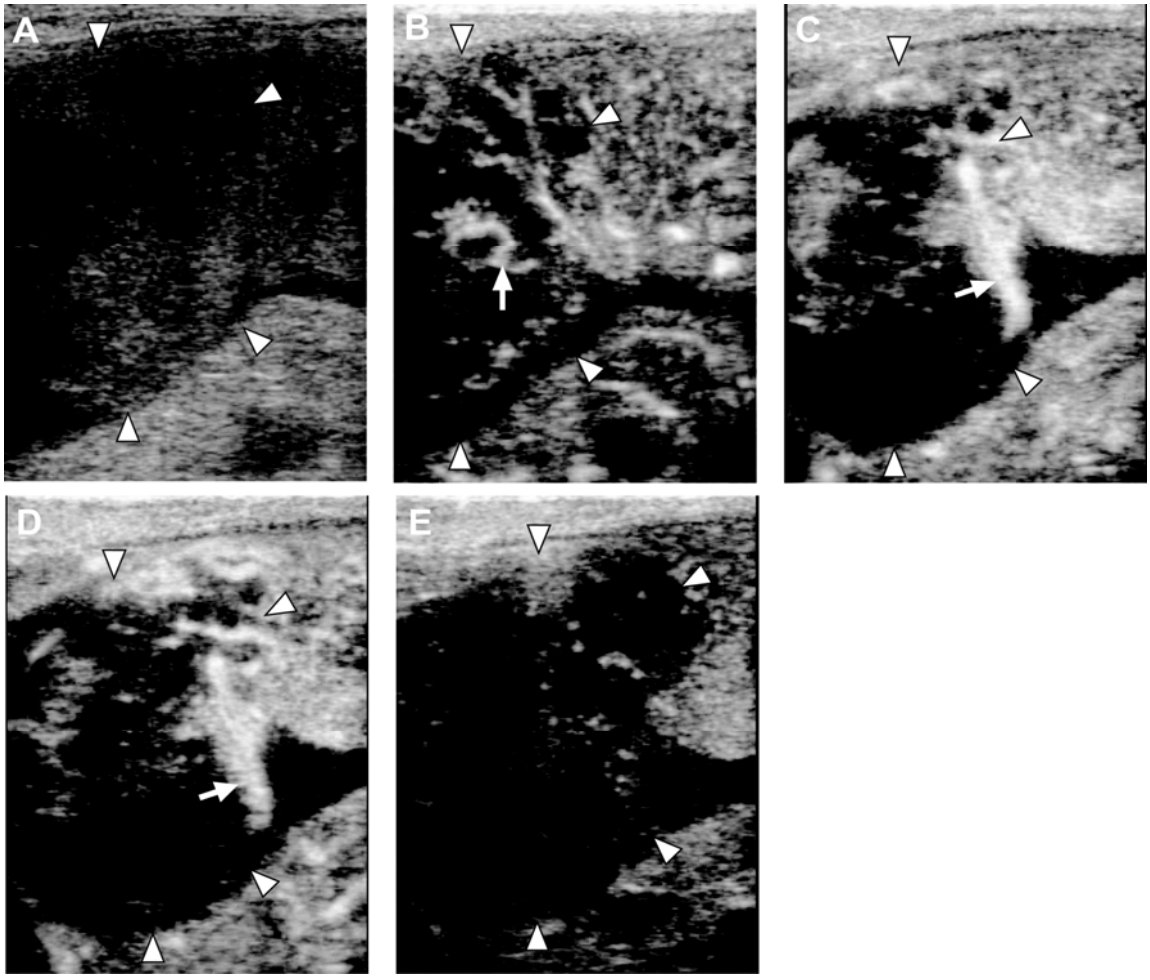

Fig. 11. (A) Conventional ultrasound imaging and (B-E) Sonazoid®-enhanced imagings of splenic hemangiosarcoma. During the early vascular phase, (B) the tortuous vessel (arrow) and (C) aberrant wide vessel (arrow) were visualized, but the entire lesion was hypoechoic (arrowheads). (D) During the late vascular phase, the lesion remained hypoechoic (arrowheads) with visualization of vessels (arrow). (E) During the parenchymal phase, the lesion became hypoechoic (arrowheads).

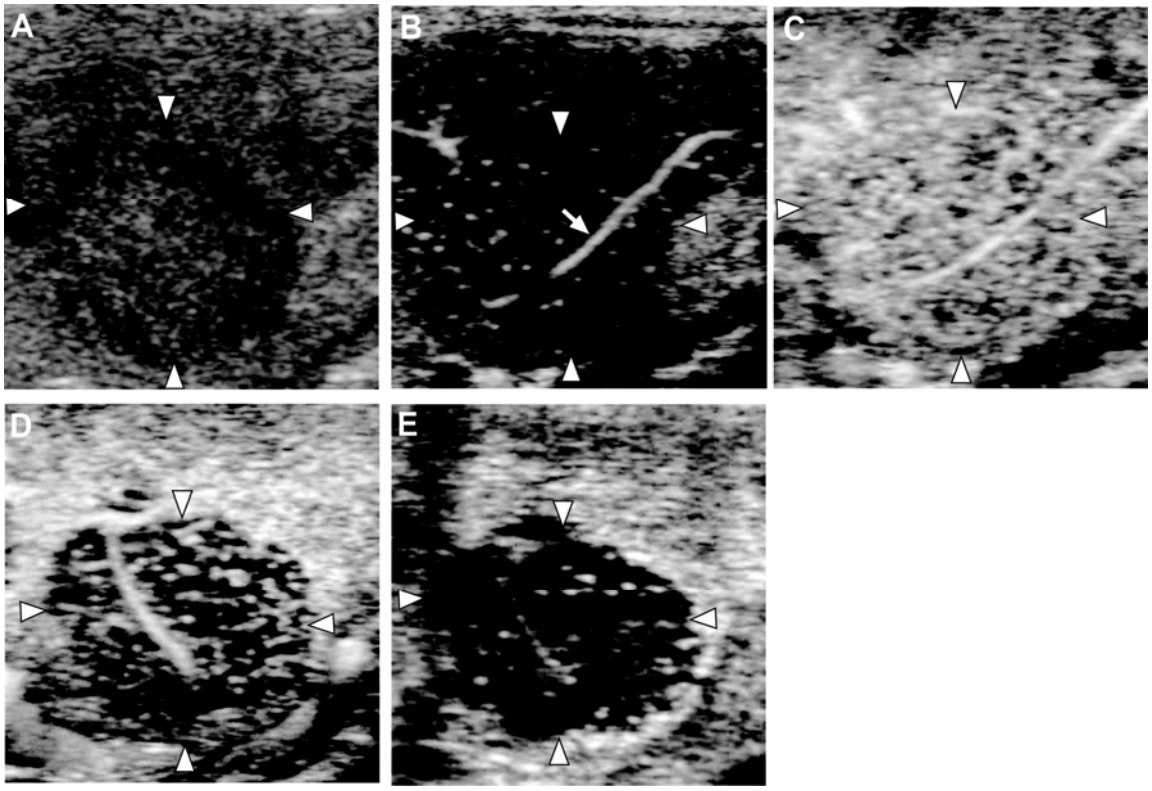

Fig. 12. (A) Conventional ultrasound imaging and (B-E) Sonazoid®-enhanced imagings of carcinoma in spleen. (B) Immediately after injection, the vessel pattern (arrow) in the lesion (arrowheads) was similar to the surrounding parenchyma. (C) During the early vascular phase, the lesion was isoechoic (arrowheads) compared to the surrounding normal parenchyma. (D) During the late vascular phase, the lesion became hypoechoic (arrowheads) compared to the surrounding normal parenchyma. (E) During the parenchymal phase, the lesion was hypoechoic (arrowheads).

General Conclusion

The goal of this study was to assess the clinical utility of Sonazoid®-enhanced ultrasonography for characterization of canine focal liver and splenic lesions. The findings of the present study suggest that Sonazoid®-enhanced ultrasonography is of value in differentiating between malignant lesions and benign nodules of liver and spleen with high accuracy.

In chapter 1, the author firstly established the protocol of Sonazoid®-enhanced ultrasonography for canine liver. The optimal time for the arterial imaging is the moment when the echogenicity of the portal vein began to rise. The optimal time for portal vein imaging is 1 min after injection and the optimal time for parenchymal imaging is from 7 min to 30 min after injection. Secondly, the author performed Sonazoid®-enhanced ultrasonography for clinical dogs with focal liver lesion. It was demonstrated that Sonazoid®-enhanced ultrasonography according to the protocol established in this study could be used to differentiate canine hepatic malignant tumors and benign nodules with high accuracy. Both the arterial and parenchymal imagings are useful for the differentiation.

In chapter 2, the author firstly performed qualitative assessment of Sonazoid® enhancement for the canine spleen. It was indicated that Sonazoid® enable the parenchymal imaging of canine spleen as with liver. Secondly, the author performed Sonazoid®-enhanced ultrasonography for clinical dogs with focal spleen lesion. In contrast to the finding of liver lesion, the result of this study shows that the parenchymal phase imaging of Sonazoid®-enhanced ultrasonography has no value in differentiating between malignant and benign splenic nodules. However, the early and late vascular phase imaging can be useful for the differentiation.

In conclusion, the result of the present study demonstrated that Sonazoid®-enhanced ultrasonography could differentiate benignancy and malignancy of liver and splenic lesions in dogs. For liver lesions, the arterial and parenchymal phase imaging could be useful for the differentiation. For the splenic lesions, the early vascular and late vascular phase imaging could be useful for the differentiation. Future studies may be optimized by blinding of the reviewer to the clinical data of the patients. Additionally, studies with higher numbers of patients will be necessary to validate the data. Despite these limitations, this thesis could be a huge first step towards making definitive diagnosis with this noninvasive diagnostic method, Sonazoid®-enhanced ultrasonography.

Footnotes

a. Schering AG, Berlin, Germany.

b. Daiichi-Sankyo, Tokyo, Japan.

c. Aplio XG, Toshiba Medical Systems, Tochigi, Japan.

d. PLT-704 AT, Toshiba Medical Systems, Tochigi, Japan

e. ImageJ, US National Institutes of Health, http://rsb.info.gov/nih-image.

f. StatMate®, ATMS, Tokyo, Japan.

g. PSK-375 BT, Toshiba Medical Systems, Tochigi, Japan.

References

1. Lamb, C. R. (1990) Abdominal ultrasonography in small animals: Examination of the liver, spleen and pancreas. *J. Small Anim. Pract*., **31**: 5-14.

2. Cuccovillo, A. and Lamb, C. R. (2002) Cellular features of sonographic target lesions of the liver and spleen in 21 dogs and a cat. *Vet. Radiol. Ultrasound,* **43**: 275-278.

3. Shinmura, R., Matsui, O., Kadoya, M., Kobayashi, S., Terayama, N., Sanada, J., Demachi, H. and Gabata, T. (2008) Detection of hypervascular malignant foci in borderline lesions of hepatocellular carcinoma: comparison of dynamic multi-detector row CT, dynamic MR imaging and superparamagnetic iron oxide-enhanced MR imaging. *Eur. Radiol*., **18**: 1918-1924.

4. Clifford, C. A., Pretorius, E. S., Weisse, C., Sorenmo, K. U., Drobatz, K. J., Siegelman, E. S. and Solomon, J. A. (2004) Magnetic resonance imaging of focal splenic and hepatic lesions in the dog. *J. Vet. Intern. Med*., **18**: 330-338.

5. Lu, M. D., Yu, X. L., Li, A. H., Jiang, T. A., Chen, M. H., Zhao, B. Z., Zhou, X. D. and Wang, J. R. (2007) Comparison of contrast-enhanced ultrasonography and contrast-enhanced CT or MRI in monitoring percutaneous thermal ablation procedure in patients with hepatocellular carcinoma: a multi-center study in China. *Ultrasound Med. Biol*., **33**: 1736-1749.

6. Blomley, M. J., Albrecht, T., Cosgrove, D. O., Eckersley, R. J., Butler-Barnes, J., Jayaram, V., Patel, N., Heckemann, R. A., Bauer, A. and Schlief, R. (1999) Stimulated acoustic emission to image a late liver and spleen-specific phase of Levovist in normal volunteers and patients with and without liver disease. *Ultrasound Med. Biol*., **25**: 1341-1352.

7. Forsberg, F., Goldberg, B. B., Liu, J., Merton, D. A., Rawool, N. M. and Shi, W. T. (1999) Tissue-specific US contrast agent for evaluation of hepatic and splenic parenchyma. *Radiology,* **210**: 125-132.

8. Lim, A. K., Patel, N., Eckersley, R. J., Taylor-Robinson, S. D., Cosgrove, D. O. and Blomley, M. J. (2004) Evidence for spleen-specific uptake of a microbubble contrast agent: a quantitative study in healthy volunteers. *Radiology,* **231**: 785-788.

9. Catalano, O., Sandomenico, F., Matarazzo, I. and Siani, A. (2005) Contrast- enhanced sonography of the spleen. *Am. J. Roentgenol*., **184**: 1150-1156.

10. Görg, C. (2007) The forgotten organ: contrast enhanced sonography of the spleen. *Eur. J. Radiol*., **64**: 189-201.

11. Kudo, M. (2007) New sonographic techniques for the diagnosis and treatment of hepatocellular carcinoma. *Hepatol. Res.,* **37** Suppl. 1: 193-199.

12. von Herbay, A., Vogt, C. and Häussinger, D. (2002) Late-phase pulse-inversion sonography using the contrast agent Levovist: differentiation between benign and malignant focal lesions of the liver. *Am. J. Roentgenol*., **179**: 1273-1279.

13. Heckemann, R. A., Cosgrove, D. O., Blomley, M. J., Eckersley, R. J., Harvey, C. J. and Mine, Y. (2000) Liver lesions: intermittent second-harmonic gray-scale US can increase conspicuity with microbubble contrast material-early experience. *Radiology,* **216**: 592-596.

14. Watanabe, R., Matsumura, M., Chen, C. J., Kaneda, Y., Ishihara, M. and Fujimaki, M. (2003) Gray-scale liver enhancement with Sonazoid (NC100100), a novel ultrasound contrast agent; detection of hepatic tumors in a rabbit model. *Biol. Pharm. Bull*., **26**: 1272-1277.

15. Watanabe, R., Matsumura, M., Chen, C. J., Kaneda, Y. and Fujimaki, M. (2005) Characterization of tumor imaging with microbubble-based ultrasound contrast agent, Sonazoid, in rabbit liver. *Biol. Pharm. Bull*., **28**: 972-977.

16. Hatanaka, K., Kudo, M., Minami, Y., Ueda, T., Tatsumi, C., Kitai, S., Takahashi, S., Inoue, T., Hagiwara, S., Chung, H., Ueshima, K. and Maekawa, K. (2008) Differential diagnosis of hepatic tumors: value of contrast-enhanced harmonic sonography using the newly developed contrast agent, Sonazoid. *Intervirology,* **5**: 61-69.

17. Hatanaka, K., Kudo, M., Minami, Y. and Maekawa, K. (2008) Sonazoid-enhanced ultrasonography for diagnosis of hepatic malignancies: comparison with contrast-enhanced CT. *Oncology,* **75** Suppl. 1: 42-47.

18. Inoue, T., Kudo, M., Hatanaka, K., Takahashi, S., Kitai, S., Ueda, T., Ishikawa, E., Hagiwara, S., Minami, Y., Chung, H., Ueshima, K. and Maekawa, K. (2008) Imaging of hepatocellular carcinoma: qualitative and quantitative analysis of postvascular phase contrast-enhanced ultrasonography with sonazoid. Comparison with superparamagnetic iron oxide magnetic resonance images. *Oncology,* **75** Suppl. 1: 48-54.

19. Ziegler, L. E., O'Brien, R. T., Waller, K. R. and Zagzebski, J. A. (2003) Quantitative contrast harmonic ultrasound imaging of normal canine liver. *Vet. Radiol. Ultrasound,* **44**: 451-454.

20. O'Brien, R. T., Iani, M., Matheson, J., Delaney, F. and Young, K. (2004) Contrast harmonic ultrasound of spontaneous liver nodules in 32 dogs. *Vet. Radiol. Ultrasound,* **45**: 547-553.

21. Nyman, H. T., Kristensen, A. T., Kjelgaard-Hansen, M. and McEvoy, F. J. (2005) Contrast-enhanced ultrasonography in normal canine liver. Evaluation of imaging and safety parameters. *Vet. Radiol. Ultrasound,* **46**: 243-250.

22. Kutara, K., Asano, K., Kito, A., Teshima, K., Kato, Y., Sasaki, Y., Edamura, K., Shibuya, H., Sato, T., Hasegawa, A. and Tanaka, S. (2006) Contrast harmonic imaging of canine hepatic tumors. *J. Vet. Med. Sci*., **68**: 433-448.

23. O'Brien, R. T. (2007) Improved detection of metastatic hepatic hemangiosarcoma nodules with contrast ultrasound in three dogs. *Vet. Radiol. Ultrasound,* **48**: 146-148.

24. Ohlerth, S., Ruefli, E., Poirier, V., Roos, M. and Kaser-Hotz, B. (2007) Contrast harmonic imaging of the normal canine spleen. *Vet. Radiol. Ultrasound,* **48**: 451-456.

25. Waller, K. R., O'Brien, R. T. and Zagzebski, J. A. (2007) Quantitative contrast ultrasound analysis of renal perfusion in normal dogs. *Vet. Radiol. Ultrasound,* **48**: 373-377.

26. Rossi, F., Leone, V. F., Vignoli, M., Laddaga, E. and Terragni, R. (2008) Use of contrast-enhanced ultrasound for characterization of focal splenic lesions. *Vet. Radiol. Ultrasound,* **49**: 154-164.

27. Kanemoto, H., Ohno, K., Nakashima, K., Takahashi, M., Fujino, Y. and Tsujimoto, H. (2008) Vascular and Kupffer imaging of canine liver and spleen using the new contrast agent Sonazoid. *J. Vet. Med. Sci*., **70**: 1265-1268.

28. Kanemoto, H., Ohno, K., Nakashima, K., Takahashi, M., Fujino, Y., Nishimura, R. and Tsujimoto, H. (2009) Characterization of canine focal liver lesions with contrast-enhanced ultrasound using a novel contrast agent−Sonazoid. *Vet. Radiol. Ultrasound,* **50**: 188-194.

29. Ivancić, M., Long, F. and Seiler, G. S. (2009) Contrast harmonic ultrasonography of splenic masses and associated liver nodules in dogs. *J. Am. Vet. Med. Assoc*., **234**: 88-94.

30. Nicolau, C. and Brú, C. (2004) Focal liver lesions: evaluation with contrast-enhanced ultrasonography. *Abdom. Imaging,* **29**: 348-359.

31. Nicolau, C., Vilana, R., Catalá, V., Bianchi, L., Gilabert, R., García, A. and Brú, C. (2006) Importance of evaluating all vascular phases on contrast-enhanced sonography in the differentiation of benign from malignant focal liver lesions. *Am. J. Roentgenol*., **186**: 158-167.

32. von Herbay, A., Vogt, C., Willers, R. and Häussinger, D. (2004) Real-time imaging with the sonographic contrast agent SonoVue: differentiation between benign and malignant hepatic lesions. *J. Ultrasound Med*., **23**: 1557-1568.

33. Lencioni, R., Piscaglia, F. and Bolondi, L. (2008) Contrast-enhanced ultrasound in the diagnosis of hepatocellular carcinoma. *J. Hepatol*., **48**: 848-857.

34. Watanabe, R., Matsumura, M., Munemasa, T., Fujimaki, M. and Suematsu, M. (2007) Mechanism of hepatic parenchyma-specific contrast of microbubble-based contrast agent for ultrasonography: microscopic studies in rat liver. *Invest. Radiol*., **42**: 643-651.

35. Iijima, H., Sasaki, S., Moriyasu, F., Suzuki, S., Yoshida, M., Horibe, T. and Tsuchiya, K. (2007) Dynamic US contrast study of the liver: Vascular and delayed parenchymal phase. *Hepatol. Res*., **37**: 27-34.

36. Liu, K., He, X., Lei, X. Z., Zhao, L. S., Tang, H., Liu, L. and Lei, B. J. (2003) Pathomorphological study on location and distribution of Kupffer cells in hepatocellular carcinoma. *World J. Gastroenterol*., **9**: 1946-1949.

37. Tanaka, M., Nakashima, O., Wada, Y., Kage, M. and Kojiro, M. (1996) Pathomorphological study of Kupffer cells in hepatocellular carcinoma and hyperplastic nodular lesions in the liver. *Hepatology,* **24**: 807-812.

38. Inoue, T., Kudo, M., Maenishi, O., Komuta, M., Nakashima, O., Kojiro, M. and Maekawa, K. (2009) Value of liver parenchymal phase contrast-enhanced sonography to diagnose premalignant and borderline lesions and overt hepatocellular carcinoma. *Am. J. Roentgenol*., **192**: 698-705.

39. Fife, W. D., Samii, V. F., Drost, W. T., Mattoon, J. S. and Hoshaw-Woodard, S. (2004) Comparison between malignant and nonmalignant splenic masses in dogs using contrast-enhanced computed tomography. *Vet. Radiol. Ultrasound,* **45**: 289-297.

40. Nyland, T. G., Mattoon, J. S., Herrgesell, E. R. and Wisner, E. R. (2002) Spleen. pp. 128-143. In: *Small Animal Diagnostic Ultrasound*, 2nd ed. (Nyland, T. G., and Mattoon, J. S., eds.), Saunders, Philadelphia.

41. von Herbay, A., Barreiros, A. P., Ignee, A., Westendorff, J., Gregor, M., Galle, P. R. and Dietrich, C. (2009) Contrast-enhanced ultrasonography with SonoVue: differentiation between benign and malignant lesions of the spleen. *J. Ultrasound Med*., **28**: 421-434.

42. Yanagisawa, K., Moriyasu, F., Miyahara, T., Yuki, M. and Iijima, H. (2007) Phagocytosis of ultrasound contrast agent microbubbles by Kupffer cells. *Ultrasound Med. Biol*., **33**: 318-325.

43. Fabry, A., Benjamin, S. A. and Angleton, G. M. (1982) Nodular hyperplasia of the liver in the beagle dog. *Vet. Pathol*., **19**: 109-119.

44. Fry, M. M. and McGavin, M. D. (2007) Bone marrow, blood cells, and lymphatic system. pp. 743-832. In: *Pathologic Basis of Veterinary Disease,* 4th ed. (McGavin, M. D., and Zachary, J. F., eds.), Mosby, St. Louis.

45. Ohlerth, S., Dennler, M., Rüefli, E., Hauser, B., Poirier, V., Siebeck, N., Roos, M.

and Kaser-Hotz, B. (2008) Contrast harmonic imaging characterization of canine splenic lesions. *J. Vet. Intern. Med*., **22**: 1095-1102.

Acknowledgement

I would like to extend thanks and my appreciation to those who have encouraged me during years of graduate studies. First and foremost, I would like to express my gratitude towards my supervisor, Dr. Mitsuyoshi Takiguchi for his support, advice, and guidance throughout the duration of this thesis project.

I would like to thank Dr. Masahiro Okumura, Dr. Kenji Ochiai, Dr. Masahiro Yamasaki, Dr. Satoshi Takagi, Dr. Hiroshi Ohta, and Dr. Tomohiro Osaki for time taken to provide advice, critical comments and assistance in completing this thesis.

I also thank Mr. Noboru Sasaki, Mr. Masahiro Murakami and all members of the Laboratory of Veterinary Internal Medicine and all staffs of Veterinary Teaching Hospital for their encouragements, support and great times.

I would also like to express my gratitude to my family for their moral support and warm encouragements.

Abstract in Japanese　（要　旨）

A Study on Contrast-enhanced Ultrasonography with Second-generation Contrast Agent Sonazoid® for Diagnosis of Liver and Splenic Nodules in Dogs

（第二世代超音波造影剤ソナゾイド®を用いた造影超音波検査による犬の肝臓および脾臓腫瘤の診断に関する研究）

肝臓および脾臓は犬において悪性腫瘍の発生率が高い臓器であるが、画像診断検査により良悪性を鑑別することは多くの場合で不可能であり、病理組織検査が必須である。しかしながら近年、細網内皮系細胞であるクッパー細胞に取り込まれる性質を持つ超音波造影剤ソナゾイド®を用いることにより、人の肝臓腫瘤診断において、造影超音波検査は病理検査に匹敵する診断精度を持つことが示され、肝臓腫瘤の画像診断検査は新たなステージに到達した。一方で獣医学領域におけるソナゾイド®造影超音波検査に関する報告は極めて少なく、その有用性は不明である。そこで本研究では、犬の肝臓腫瘤診断におけるソナゾイド®造影超音波検査の精度を評価する（第一章）とともに、肝臓と同様に細網内皮系細胞を豊富に有する脾臓におけるソナゾイド®造影超音波検査の有用性を評価する（第二章）ことを目的とした。

第一章では、肝臓腫瘤を持つ犬 27 症例 28 結節に対してソナゾイド®造影超音波検査を実施した。造影所見は動脈相、門脈相および実質相それぞれにおいて、腫瘤のエコー源性を周囲の正常実質と比較して相対的に Hypo/Iso/Hyper の三群に分類した。その後、全例において病理組織学的検査もしくは細胞診を行い、病理学的診断とした。得られた造影所見から良悪性鑑別において有意（$P < 0.05$）となる所見を抽出し、各々の感度、特異度を算出した。28 結節のうち、20 結節（結節性過形成 5 例、肝細胞癌 11 例、血管肉腫 1 例、混合型肝癌 1 例、カルチノイド 1 例、骨肉腫 1 例）においては病理組織学的検査により、2 結節（結節性過形成 1 例、リンパ腫 1 例）においては細胞診により確定診断を得た。残りの 6 結節においては細胞診とその他の臨床検査所見から血管肉腫であることが強く疑われたが、確定診断には至らなかった。確定診断が得られた 22 結節に

おいて統計学的解析を実施し、動脈相および実質相の評価が良悪性鑑別に有効であることが示された。実質相においてHypoと分類された結節は有意に悪性であり、感度94%、特異度 100%で悪性と診断することが可能であった。動脈相において Hyper もしくはHypoと分類された結節は有意に悪性であり、感度93%、特異度83%で悪性と診断することが可能であった。また動脈相では多くの肝細胞癌がHyperとなったが、全ての血管肉腫で Hypo であった。以上の結果から、ソナゾイド®造影超音波検査は、極めて高い精度で犬の肝臓腫瘤の良悪鑑別を行えることが明らかとなった。さらに、動脈相の検査所見から、悪性腫瘍のより詳細な鑑別診断が可能であることが示唆された。

第二章では、超音波検査により脾臓腫瘤が確認された犬29症例を対象とした。全症例にソナゾイド®造影超音波検査を実施し、早期血管相、後期血管相、および実質相において腫瘤のエコー源性を周囲の正常実質と比較して相対的に、Hypo/Hetero/Isoの三群に分類した。その後、全例において病理学的検査を実施し、確定診断を得た。得られた造影所見から良悪性鑑別において有意（$P < 0.05$）となる所見を抽出し、各々の感度、特異度を算出した。29症例中、良性腫瘤は13例（結節性過形成8例、血腫2例、髄外造血2例、肉芽腫1例）であり、悪性腫瘍は16例（血管肉腫8例、リンパ腫3例、組織球肉腫2例、平滑筋肉腫1例、骨肉腫1例、癌腫1例）であった。統計学的解析により、早期血管相および後期血管相の評価が良悪性鑑別に有効であることが示されたが、実質相においては有意な所見は認められなかった。早期血管相においては、Hypo と分類された症例は、感度38%、特異度100%にて悪性と診断することが可能であった。後期血管相においては、Hypoと分類された症例は、感度81%、特異度85%にて悪性と診断することが可能であった。以上の結果から、ソナゾイド®造影超音波検査が犬の脾臓腫瘤の良悪性鑑別に有用であることが明らかとなった。ただし、その評価には早期および後期血管相のみが有用であり、実質相において有意な所見は認められなかった。これは、実質相の評価が良悪性鑑別において有用となる肝臓腫瘤とは著しく異なる結果であった。

本研究の成果より、犬の肝臓および脾臓腫瘤の良悪性鑑別においてソナゾイド®造影超音波検査が極めて有用であることが示された。これは、これまで病理組織学的検査に頼らざるを得なかった動物の腫瘍診断において、画像診断検査法による確定診断へと近づく大きな一歩となる。さらに今後の研究により、本法を用いて良悪性鑑別のみならず、より詳細な鑑別診断が可能となることが期待される。